

An evaluation for geometries, formation enthalpies, and dissociation energies of diatomic and triatomic (C, H, N, O), NO₃, and HNO₃ molecules from the PAW DFT method with PBE and optB88-vdW functionals (*AIP Advances*, in press, 2022)

Yong Han

Division of Chemical and Biological Sciences, Ames National Laboratory, Ames, Iowa 50011, USA.

Department of Physics and Astronomy, Iowa State University, Ames, Iowa 50011, USA.

*Email: y27h@ameslab.gov

ABSTRACT

Structural geometries, formation enthalpies, and dissociation energies of all diatomic and triatomic molecules consisting of the four basic elements C, H, N, and/or O are calculated from the projector augmented wave (PAW) density functional theory (DFT) method with the PBE and optB88-vdW exchange-correlation functionals. The calculations are also extended to two larger molecules NO₃ and HNO₃, which consist of 4 and 5 atoms, respectively. In total, 82 molecules or isomers are considered in the calculations. The geometric parameters including 42 bond lengths and 15 bond angles of these molecules from the planewave DFT method are highly satisfactory, relative to available experimental data. The error analysis is also performed for 49 formation enthalpies and 138 dissociation energies (including 51 atomization energies as well as corresponding bond dissociation energies). The results are also compared with the previous data from various atomic-orbitals-based methods for molecules and from similar or different planewave DFT methods for various solids and other molecules. This provides an informative and instructive evaluation, especially for calculating the large-size material systems containing these small molecules as well as for further developing DFT methods.

I. INTRODUCTION

Atomic-orbitals-based methods (AOBMs) [1, 2, 3] are generally regarded by the computational chemical community as more accurate numerically than the planewave density functional theory (DFT) methods [4, 5]. The reason is that, in earlier years, the pseudopotentials in the planewave DFT methods were not carefully generated when used in many planewave codes. However, since the projector augmented wave (PAW) method was suggested and used by Blöchl [6], a lot of effort has been made and the reliable PAW pseudopotentials have been generated [7] with constantly updated versions released, as implemented in the Vienna *Ab initio* Simulation Package (VASP) code [4]. Due to the high computational costs, AOBMs with higher accuracies are generally used to calculate relatively small systems like molecules. In contrast, the planewave DFT

methods can be computationally much more efficient [4, 5] by using the supercell technology with the periodic boundary conditions to simulate any crystalline materials.

Due to the fundamental importance in various scientific areas including chemical physics, biophysics, environmental science, interstellar medium, etc., research on small molecules is constantly developing both theoretically and experimentally. Specifically, adsorption of small molecules on materials surfaces (including outer surfaces of materials or the surfaces of pores in materials, e.g., molecular sieves [8, 9]) is often considered for both theoretical studies and applications. The supercell for such a system by using a planewave DFT method often contains hundreds to thousands of atoms at least for obtaining reliable adsorption properties. In addition, *ab initio* molecular dynamics (AIMD) simulations [10] for such systems are also selectively implemented for, e.g., visualizing the diffusion paths of molecules on the surfaces, while AIMD simulations are even much more demanding than normal structural optimizations. Thus, using AOBMs with higher accuracies but high computational costs is impractical for such computations. Instead, the planewave DFT methods can be computationally practical due to the high efficiency. However, when a planewave DFT method is applied to a specific system, the reliability of the method must be first assessed because the accuracy of the DFT results can significantly depend on the electronic exchange-correlation energy functionals. To this end, we mention an example. It is well-known that Perdew-Burke-Ernzerhof (PBE) functional [11] cannot predict the interlayer spacing of graphite due to the absence of the dispersion corrections, e.g., the predicted lattice constant $c = 8.870 \text{ \AA}$ along the [0001] direction of graphite from our previous PBE calculations [12] is notoriously much larger than the experimental value of 6.6720 \AA [13]. In contrast, the value of 6.701 \AA from our optB88-vdW [14] calculations with dispersion corrections can reproduce the above experimental c value very well [12]. Thus, one should be particularly careful when selecting a functional with or without dispersion corrections to calculate the weakly bonded systems like graphite.

As a semilocal functional, the generalized gradient approximation (GGA) generally has comparably good accuracies for calculating ground state properties of neither weakly bonded nor strongly correlated systems. For example, recent extensive tests on the lattice constants, bulk moduli, and cohesive energies (or atomization energies) of 44 strongly and 17 weakly bonded solids from various local, semilocal, and nonlocal functionals (so-called “DFT Jacob’s ladder”) have been reported [15, 16]. For the weakly bonded systems, dispersion corrections need to be considered [17], while for strongly correlated systems, DFT+U corrections are usually needed [18]. In addition, more nonlocal functionals (upper rungs of the DFT Jacob’s ladder) can have higher accuracies but higher computational costs than more local functionals (lower rungs). Therefore, to appropriately choose a functional before calculating a specific system, both accuracy and computational cost need to be balanced.

Recently, we have selected and applied the optB88-vdW functional [14], which typically considers dispersion correction including van der Waals (vdW) interactions, to various vdW materials with guest atoms [12, 19–30] and silica polymorphs with molecular groups consisting of C, H, and O [31]. These applications have already been proven very successful. The success is not surprising, given that these systems include weakly bonded interlayer spaces, while for the weakly bonded systems, the

GGA plus dispersion corrections generally have satisfactory accuracies, as described above. In the near future, we will extensively involve the adsorption and diffusion properties of small molecules on the outer or inner pore surfaces of such weakly bonded materials. The elements that make up these small molecules will be C, H, N and/or O, which are also 4 most fundamental elements of organisms. Before extensively calculating these large-size systems, an evaluation even only for these small molecules in gas phase will be very instructive and necessary.

In this work, we use the PAW DFT method with the optB88-vdW functional to calculate the structural geometries, formation enthalpies, and dissociation energies of all diatomic and triatomic molecules consisting of C, H, N, and/or O, by considering 80 linear or triangular molecules or isomers. Then, we extend our calculations to two larger molecules NO_3 and HNO_3 , containing 4 and 5 atoms, respectively, because these molecules will be the first candidates which will be involved in our ongoing projects for, e.g., separation of rare earth elements. As comparison, we also obtain the results using the most popular PBE GGA [11] without dispersion corrections.

The paper is organized as follows. The computational details are described in Sec. II. In Sec. III, we tabulate and discuss the structural geometries, formation enthalpies, dissociation energies, and corresponding spin states of all 82 molecular molecules or isomers consisting of C, H, N and/or O from our DFT calculations and previous experiments or AOBM calculations available in literature. In Sec. IV, we also discuss our results and make error analysis by comparing with other relevant DFT results in the literature. Sec. V provides a summary of this work. The formulation of formation enthalpies and dissociation energies is provided in Supplementary Material (SM) Sec. S1 and the original data for error analysis are also provided in SM.

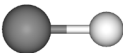
II. COMPUTATIONAL DETAILS


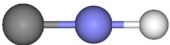
We use the VASP code [4] to perform all DFT calculations in this work, with the PAW pseudopotentials [7] developed by the VASP group and released in 2015. For the electron-electron exchange correlation part, as described in Sec. I, we use PBE and optB88-vdW functionals without and with dispersion corrections, respectively. In all DFT calculations, we take the energy cutoff to be 600 eV with sufficient accuracy (cf. the default energy cutoffs of 400 eV for C, 250 eV for H, 400 eV for N, and 400 eV for O in the PAW pseudopotential data files). Spin polarizations are always considered because the energy of a molecular configuration depends on the spin state. For 80 diatomic or triatomic molecules or isomers, the supercell is always taken to be a rectangular box with the size of $23 \text{ \AA} \times 22 \text{ \AA} \times 21 \text{ \AA}$. For two larger molecules (NO_3 and HNO_3), the supercell is taken to be slightly larger with the size of $24.3 \text{ \AA} \times 24.2 \text{ \AA} \times 24.1 \text{ \AA}$. These supercell sizes are sufficiently large so that the interactions between replicas can be ignored. The k mesh is always taken to be $1 \times 1 \times 1$ which is sufficient because of the large supercell sizes. During energy minimization, the atoms in the supercell are fully relaxed after the initial configurations are judiciously selected based on previous experiments or AOBM calculations in the literature. The convergence of total energy is reached when the force exerted on each atom is less than 0.01 eV/\AA .

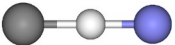
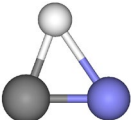
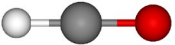

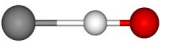
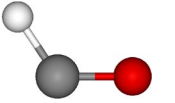
III. RESULTS AND DISCUSSION

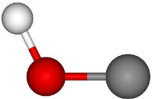
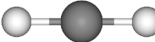

In Table I, we list our PAW PBE and optB88-vdW results for all diatomic and triatomic molecules or isomers consisting of C, H, N, and/or O. As comparison, the corresponding AOBM and experimental data available in the previous literature are also listed. The theoretical and experimental data for two larger molecules NO_3 and HNO_3 are listed in Table II.

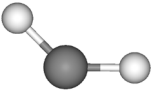
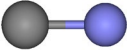

TABLE I. Theoretical and experimental data for 82 diatomic and triatomic molecules or isomers consisting of C, H, N, and/or O. Molecular formulas adopt the NIST notations [32] for convenient indexing, where molecules are listed in alphabetic order of element symbols and the numbers of elemental atoms in the molecule as subscripts 1, 2, 3, ..., etc., but the conventional notations and names for molecules or isomers are also listed. All ball-and-stick geometric structures are from our PAW optB88-vdW calculations with the gray, white, blue, and red balls representing C, H, N, and O atoms, respectively. “PBE” and “optB88” are our PAW DFT calculations with PBE and optB88-vdW functionals, respectively. The results from other functionals in the previous literature (see Sec. IV) are not provided in this list, except for a few specific molecules or isomers. “AOBM” denotes the data from various atomic-orbitals-based methods in the literature. “Exp.” denotes available experiment data from the literature. M (in unit of Bohr magneton μ_B) is the spin magnetic moment of the molecule and taken to be the value with the lowest energy for a given configuration. $l_{\alpha\beta}$ (in Å) is the bond length (or interatomic distance or atomic spacing) between atom α and atom β . $\theta_{\alpha\beta\gamma}$ (in degree $^\circ$) is the angle between $l_{\beta\alpha}$ and $l_{\beta\gamma}$. ΔH_f (in eV) is the formation enthalpy from Eq. (S2). $D_{p1+p2+p3+\dots}$ (in eV) is the dissociation energy for products p1, p2, p3, ... from Eq. (S4). The dissociation energy in the final column is also called the atomization energy from Eq. (S6). The data for ΔH_f and $D_{p1+p2+p3+\dots}$ are obtained always at 0 K. Under the corresponding values in eV, the available experimental data from Active Thermochemical Tables (ATcT) [33] for ΔH_f and $D_{p1+p2+p3+\dots}$ in units of kJ/mol with the uncertainties are also listed, as indicated by “ \pm ”, corresponding to estimated 95% confidence limits [34, 35]. The species names from ATcT [33] are adopted partly.



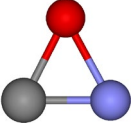
Formula: C_1H_1		M	ΔH_f	$D_{\text{C+H}}$
CH or HC (Methyldiyne)		l_{CH}		
	PBE	1 1.1369	6.429	3.697
	optB88	1 1.1300	6.384	3.895
	AOBM [36]	1.1204		
	Exp. [37]	1.1199		
	Exp. [38]	1.119786		


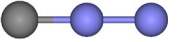
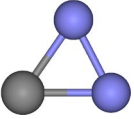
Exp.		[33]			6.14432			3.46791		
					592.837±0.097			334.602±0.087		
Formula: C ₁ H ₁ N ₁			<i>M</i>			ΔH_f	$D_{\text{CH+N}}$	$D_{\text{CN+H}}$	$D_{\text{C+HN}}$	$D_{\text{C+H+N}}$
Linear HCN or NCH (Hydrogen cyanide)			l_{CH}	l_{CN}						
	PBE	0	1.0749	1.1611	1.240	10.386	5.544	10.220	14.083	
	optB88	0	1.0699	1.1561	1.336	10.311	5.765	10.181	14.206	
	AOBM	[39]	1.067	1.160						
	AOBM	[40]	1.0651-1.0826	1.1527-1.1758						
	Exp.	[41]	1.06549	1.15321						
	Exp.	[33]				1.34402	9.6775	5.4215	9.7473	13.14542
					129.678±0.089	933.74±0.12	523.09±0.12	940.47±0.18	1268.340±0.085	
Linear HNC or CNH (Hydrogen isocyanide)			l_{NH}	l_{NC}						
	PBE	0	1.0050	1.1774	1.857	9.769	4.927	9.603	13.466	
	optB88	0	1.0019	1.1728	1.946	9.701	5.155	9.571	13.596	
	AOBM	[39]	0.996	1.175						
	AOBM	[40]	0.9952-1.0063	1.1686-1.1895						
	Exp.	[42]	0.9940	1.1689						
	Exp.	[33]				1.9906	9.0310	4.7749	9.1008	12.4989
					192.06±0.32	871.36±0.32	460.71±0.32	878.09±0.35	1205.96±0.31	
Linear CHN or NHC			l_{HC}	l_{HN}						
PBE	0	1.1043	1.0155	11.553	0.072	-4.769	-0.094	3.769		

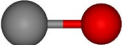

	optB88	0	1.1054	1.0178		11.633	0.014	-4.532	-0.116	3.909
Triangular (cyclic) HCN or CHN, etc.			l_{CH}	l_{CN}	θ_{HCN}					
	PBE	0	1.2016	1.1961	70.16	3.225	8.400	3.559	8.234	12.097
	optB88	0	1.2082	1.1911	69.76	3.349	8.299	3.752	8.168	12.193
	AOBM [39]		1.186	1.195	71.67					
	AOBM [40]		1.1835- 1.2017	1.1867- 1.2089	71.623- 71.827					
Formula: $\text{C}_1\text{H}_1\text{O}_1$		M				ΔH_f	$D_{\text{CH}+\text{O}}$	$D_{\text{CO}+\text{H}}$	$D_{\text{C}+\text{HO}}$	$D_{\text{C}+\text{H}+\text{O}}$
Linear HCO or OCH			l_{CH}	l_{CO}						
	PBE	1	1.0728	1.1944		1.456	7.997	0.191	6.987	11.694
	optB88	1	1.0685	1.1928		1.540	7.843	0.239	6.851	11.738
Linear HOC or COH			l_{OH}	l_{OC}						
	PBE	1	6.6239	1.1431		1.648	7.805	0.000	6.796	11.502
	optB88	1	6.6164	1.1394		1.779	7.605	0.000	6.613	11.500
Linear CHO or OHC			l_{HC}	l_{HO}						
	PBE	1	1.3356	1.0108		8.153	1.300	-6.505	0.291	4.997
	optB88	1	1.5686	1.0051		8.259	1.125	-6.479	0.133	5.020
Triangular HCO or OCH (Formyl)			l_{CH}	l_{CO}	θ_{HCO}					
	PBE	1	1.1337	1.1882	123.91	0.465	8.988	1.183	7.979	12.685
	optB88	1	1.1294	1.1860	123.88	0.534	8.850	1.245	7.858	12.744
	AOBM [43]		1.112- 1.1462	1.1729- 1.1952	123.79- 125.02	0.396-0.481		0.607-0.824		11.730-12.105

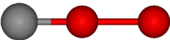
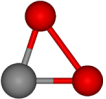
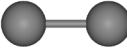
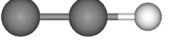
	Exp.	[44]	1.1102	1.17115	127.426						
	Exp.	[45]	1.125	1.175	124.95						
	Exp.	[46]	1.1514	1.17708	123.01						
	Exp.	[47]	1.1191	1.1754	124.43						
	Exp.	[33]				0.42888	8.2738	0.63066	7.3308	11.74169	
						41.381±0.096	798.30±0.13	60.849±0.095	707.31±0.10	1132.901±0.097	
Triangular HOC or COH (Isoformyl)			l_{OH}	l_{OC}	θ_{HOC}						
	PBE		1	1.0070	1.2755	115.98	2.304	7.149	-0.656	6.140	10.846
	optB88		1	1.0058	1.2744	116.30	2.352	7.032	-0.573	6.040	10.926
	AOBM	[48]		0.980	1.299	111.7					
	AOBM	[49]		0.97604	1.27300	112.956					
	Exp.	[33]				2.2516	6.4510	-1.1921	5.5080	9.9190	
						217.25±0.69	622.43±0.69	-115.02±0.68	531.44±0.68	957.04±0.68	
Formula: C ₁ H ₂			M			ΔH_f	D_{CH+H}	D_{H_2+C}		D_{C+2H}	
Linear HCH			l_{CH}	l_{CH}							
	PBE		2	1.0740	1.0730	4.078	4.620	3.780		8.317	
	optB88		2	1.0700	1.0702	4.368	4.510	3.416		8.405	
Linear CHH or HHC			l_{HC}	l_{HH}							
	PBE		2	1.4844	0.7812	7.635	1.063	0.222		4.760	
	optB88		2	1.6136	0.7648	7.704	1.174	0.080		5.069	
Triangular HCH (Methylene)			l_{CH}	l_{CH}	θ_{HCH}						
	PBE		2	1.0849	1.0849	135.06	3.890	4.808	3.967	8.505	

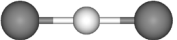
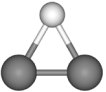
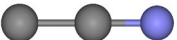
	optB88	2	1.0816	1.0816	135.04	4.176	4.702	3.608	8.597
	AOBM [50]		1.07481	1.07481	133.839				
	Exp. [51]		1.07530	1.07530	133.9308				
	Exp. [33]					4.05299	4.3304	3.32019	7.79826
						391.054±0.096	417.82±0.11	320.350±0.089	752.418±0.089
Formula: C ₁ N ₁		<i>M</i>				ΔH_f	D_{C+N}		
CN or NC (Nitrilomethyl)			l_{CN}						
	PBE	1	1.1768			4.515			8.539
	optB88	1	1.1733			4.606			8.441
	AOBM [52]		1.18						
	B3LYP [53]		1.162						
	Exp. [37]		1.1718						
	Exp. [33]					4.5264			7.7240
						436.73±0.14			745.25±0.13
Formula: C ₁ N ₁ O ₁		<i>M</i>			ΔH_f	D_{CN+O}	D_{CO+N}	D_{C+NO}	D_{C+N+O}
Linear NCO or OCN (Cyanooxidanyl)			l_{CN}	l_{CO}					
	PBE	1	1.2343	1.1932	1.067	6.471	3.508	7.736	15.010
	optB88	1	1.2292	1.1914	1.139	6.467	3.409	7.592	14.908
	AOBM [54]		1.241	1.182					
	AOBM [55]		1.2330	1.1851					
	AOBM [56]		1.223	1.177					
	Exp. [57]		1.200	1.206					

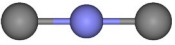
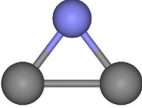

	Exp.	[33]			1.3156	5.7691	2.3820	6.9969	13.4931
					126.94±0.33	556.63±0.35	229.83±0.33	675.10±0.33	1301.89±0.33
Linear NOC or CON			l_{OC}	l_{ON}					
	PBE	1	1.2084	1.3038	6.023	1.516	-1.448	2.780	10.054
	optB88	1	1.2008	1.3225	6.043	1.563	-1.495	2.689	10.005
	AOBM	[54]	1.211	1.303					
	AOBM	[55]	1.1948	1.3306					
	AOBM	[56]	1.184	1.325					
Linear CNO or ONC (Nitrosomethylidyne)			l_{NC}	l_{NO}					
	PBE	1	1.2245	1.2237	3.645	3.894	0.930	5.158	12.433
	optB88	1	1.2186	1.2269	3.731	3.875	0.817	5.001	12.316
	AOBM	[54]	1.226	1.221					
	AOBM	[55]	1.2168	1.2223					
	AOBM	[56]	1.210	1.216					
	Exp.	[33]			4.035	3.049	-0.338	4.277	10.774
					389.3±1.1	294.2±1.0	-32.6±1.0	412.7±1.0	1039.5±1.0
Triangular (cyclic) NCO or OCN (Oxazirinyl)			l_{CN}	l_{CO}	θ_{NCO}				
	PBE	1	1.3467	1.4224	62.62	4.455	3.084	0.121	4.349
	optB88	1	1.3396	1.4278	63.05	4.553	3.053	-0.005	4.179
	AOBM	[54]	1.349	1.467	59.54				
	AOBM	[55]	1.3457	1.3937	63.92				
	AOBM	[56]	1.344	1.380	63.70				

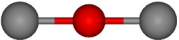
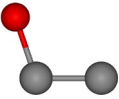

	Exp.	[33]				4.665	2.420	-0.967	10.14	
						450.1±1.5	233.5±1.4	-93.3±1.4	978.7±1.4	
Formula: C ₁ N ₂			<i>M</i>			ΔH_f	$D_{\text{CN+N}}$	$D_{\text{C+N}_2}$	$D_{\text{C+2N}}$	
Linear NCN (Methanetetraylbisamidogen)			l_{CN}	l_{CN}						
	PBE		2	1.2363	1.2363	4.149	5.562	3.708	14.101	
	optB88		2	1.2321	1.2321	4.301	5.569	3.484	14.010	
	B3LYP	[58]		1.232	1.232					
	B3LYP	[59]		1.225	1.225					
	Exp.	[33]				4.6768	4.7268	2.6964	12.4508	
						451.24±0.44	456.07±0.44	260.16±0.43	1201.32±0.43	
Linear CNN or NNC (Diazomethylene)			l_{NC}	l_{NN}						
	PBE		2	1.2566	1.1999	5.308	4.404	2.550	12.942	
	optB88		2	1.2496	1.1931	5.484	4.386	2.300	12.827	
	AOBM	[60]		1.2325	1.2158					
	AOBM	[60]		1.2526	1.2241					
	B3LYP	[58]		1.233	1.198					
	Exp.	[33]				6.004	3.399	1.369	11.123	
						579.3±3.8	328.0±3.7	132.1±3.7	1073.2±3.7	
Triangular (cyclic) NCN (3H-Diazirin-3-ylidene)			l_{CN}	l_{CN}	θ_{NCN}					
	PBE		0	1.4036	1.4036	54.98	5.733	3.978	2.124	12.517
	optB88		0	1.4023	1.4018	54.93	5.887	3.982	1.897	12.424
	AOBM	[60]		1.4100	1.4100	54.9101				

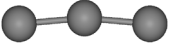
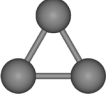
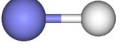

	AOBM	[60]		1.3979	1.3979	55.0543			
	B3LYP	[61]		1.387	1.387	54.9			
	Exp.	[33]				6.002	3.403	1.372	11.126
						579.1±2.7	328.3±2.7	132.4±2.7	1073.5±2.7
Formula: C ₁ O ₁			<i>M</i>			ΔH_f			D_{C+O}
CO or OC (Carbon monoxide)				l_{CO}					
	PBE		0	1.1431		-0.621			11.502
	optB88		0	1.1393		-0.715			11.499
	AOBM	[62]		1.1513					
	Exp.	[37]		1.128323					
	Exp.	[33]				-1.17950			11.11104
						-113.804±0.026			1072.052±0.046
Formula: C ₁ O ₂			<i>M</i>			ΔH_f	D_{CO+O}	D_{C+O_2}	D_{C+2O}
Linear OCO (Carbon dioxide)				l_{CO}	l_{CO}				
	PBE		0	1.1764	1.1764	-3.870	6.273	11.727	17.775
	optB88		0	1.1739	1.1738	-3.863	6.148	11.648	17.647
	AOBM	[63]		1.15	1.15				
	Exp.	[64]		1.162	1.162				
	Exp.	[33]				-4.07430	5.45315	11.44748	16.56419
						-393.110±0.015	526.149±0.024	1104.514±0.043	1598.201±0.043
Linear COO or OOC (Dioxymethylidyne)				l_{OC}	l_{OO}				
	PBE		0	1.1797	1.3236	3.048	-0.645	4.809	10.857

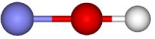

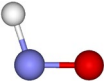
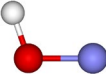
	optB88	0	1.1739	1.3421	2.975	-0.690	4.809	10.809	
	Exp. [33]				3.107	-1.729	4.266	9.383	
					299.8±1.7	-166.8±1.6	411.6±1.6	905.3±1.6	
Triangular OCO (Dioxiranylidene)			l_{CO}	l_{CO}	θ_{OCO}				
	PBE	0	1.3404	1.3403	71.21	2.198	0.205	5.660	11.707
	optB88	0	1.3397	1.3399	71.69	2.158	0.127	5.627	11.626
	Exp. [33]				1.972	-0.594	5.401	10.518	
					190.3±1.4	-57.3±1.4	521.1±1.4	1014.8±1.4	
Formula: C ₂		M			ΔH_f			D_{2C}	
CC (Ethyne)			l_{CC}						
	PBE	2	1.3142		8.780			6.935	
	optB88	2	1.3093		8.865			6.704	
	AOBM [65]		1.248-1.255						
	AOBM [66]		1.247, 1.254					6.072-6.371	
	Exp. [37]		1.2425						
	Exp. [33]				8.49875			6.24762	
					820.005±0.092			602.804±0.028	
Formula: C ₂ H ₁		M			ΔH_f	D_{C+CH}	D_{C_2+H}	D_{2C+H}	
Linear CCH (Ethyne)			l_{CC}	l_{CH}					
	PBE	1	1.2113	1.0720	5.938	8.348	5.110	12.045	
	optB88	1	1.2065	1.0675	6.175	7.993	5.184	11.888	

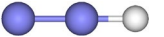

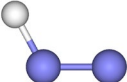
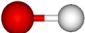
	AOBM	[67]		1.223	1.075				
	Exp.	[68]		1.21652	1.04653				
	Exp.	[33]				5.8430	7.6745	4.8948	11.1424
						563.76±0.15	740.48±0.15	472.28±0.13	1075.08±0.13
<hr/>									
Linear CHC				l_{HC}	l_{HC}				
	PBE		1	1.1967	1.2014	12.903	1.383	-1.854	5.080
	optB88		1	1.1922	1.2018	13.054	1.114	-1.695	5.009
<hr/>									
Triangular (cyclic) CHC or CCH or HCC				l_{HC}	l_{HC}	θ_{HCH}			
	PBE		1	1.2853	1.2789	59.94	6.750	7.536	4.299
	optB88		1	1.2897	1.2809	59.50	7.016	7.152	4.343
<hr/>									
Formula: C ₂ N ₁			M			ΔH_f	$D_{\text{C+CN}}$	$D_{\text{C}_2+\text{N}}$	$D_{2\text{C}+\text{N}}$
Linear CCN or NCC (Cyanomethylidyne)				l_{CC}	l_{CN}				
	PBE		1	1.3743	1.1972	6.929	5.443	7.047	13.982
	optB88		1	1.3684	1.1920	6.966	5.425	7.162	13.866
	AOBM	[60]		1.4152	1.1993				
	AOBM	[60]		1.3908	1.1811				
	AOBM	[69]		1.4045	1.1889				
	AOBM	[70]		1.3821	1.1847				
	Exp.	[33]				7.096	4.803	6.280	12.527
						684.7±2.1	463.4±2.0	605.9±2.0	1208.7±2.0
<hr/>									
Linear CNC (Isocyanomethylidyne)				l_{NC}	l_{NC}				


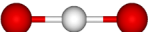
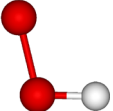
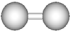
	PBE	1	1.2529	1.2531		6.873	5.499	7.103	14.038
	optB88	1	1.2481	1.2482		6.892	5.499	7.236	13.940
	AOBM [60]		1.2658	1.2658					
	AOBM [60]		1.2479	1.2479					
	AOBM [69]		1.2534	1.2534					
	AOBM [70]		1.2462	1.2462					
	Exp. [71]		1.245	1.245					
	Exp. [33]					6.967	4.933	6.409	12.657
					672.2±1.7	476.0±1.7	618.4±1.7	1221.2±1.7	
Triangular (cyclic) CNC (2,3-didehydro-1H-azirin-1-yl)			l_{NC}	l_{NC}	θ_{CNC}				
	PBE	1	1.3188	1.3188	72.73	7.375	4.997	6.601	13.536
	optB88	1	1.3129	1.3118	74.10	7.531	4.860	6.597	13.301
	AOBM [60]		1.3275	1.3275	74.5919				
	AOBM [60]		1.3099	1.3099	75.7304				
	Exp. [33]					7.465	4.434	5.910	12.157
					720.3±2.1	427.8±2.0	570.2±2.0	1173.0±2.0	
Formula: C ₂ O ₁		M				ΔH_f	$D_{\text{C+CO}}$	$D_{\text{C}_2+\text{O}}$	$D_{2\text{C}+\text{O}}$
Linear CCO or OCC (Dicarbon monoxide)			l_{CC}	l_{CO}					
	PBE	2	1.3705	1.1785		3.876	3.360	7.928	14.862
	optB88	2	1.3625	1.1770		3.991	3.079	7.874	14.578
	AOBM [72]		a=1.3699	b=1.1627					



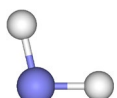
	AOBM	[73]	a=1.3718	b=1.1638					
	AOBM	[74]	a=1.373	b=1.169					
	AOBM	[75]	a=1.388	b=1.149					
	Exp.	[33]			3.9086	2.2851	7.1486	13.3961	
					377.12±0.83	220.48±0.82	689.73±0.82	1292.53±0.82	
Linear COC			l_{oc}	l_{oc}					
	PBE		2	1.2689	1.2690	6.501	0.735	5.302	12.237
	optB88		2	1.2675	1.2669	6.575	0.494	5.290	11.993
	Exp.	[33]			6.768	-0.574	4.289	10.536	
					653.0±1.5	-55.4±1.5	413.8±1.5	1016.6±1.5	
Triangular CCO or OCC			l_{cc}	l_{co}	θ_{cco}				
	PBE		2	1.3646	1.3540	109.03	5.957	1.280	5.847
	optB88		2	1.3598	1.3511	108.66	6.008	1.061	5.857
Formula: C ₃			M			ΔH_f		D_{C+C_2}	D_{3C}
Linear CCC (1,2-Propadiene-1,3-diyliidene)			l_{cc}	l_{cc}					
	PBE		0	1.3018	1.3019	8.706	7.932		14.866
	optB88		0	1.2948	1.2948	8.658	7.991		14.695
	AOBM	[76]		1.29452	1.29452				
	Exp.	[77]		1.29471	1.29471				
	Exp.	[33]				8.4422	7.4297		13.6774
						814.55±0.53	716.86±0.51		1319.67±0.51
Triangular (quasilinear) CCC			l_{cc}	l_{cc}	θ_{ccc}				

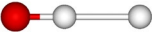

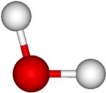
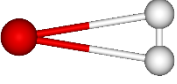
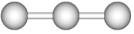
	PBE	0	1.3027	1.3028	149.25	8.700	7.937	14.872	
	optB88	0	1.2949	1.2949	170.24	8.658	7.991	14.695	
	AOBM [78]		1.289664	1.289664	161.6				
Triangular (cyclic) CCC (2-Cyclopropyn-1-ylidene)			l_{CC}	l_{CC}	θ_{CCC}				
	PBE	2	1.3778	1.3777	59.99	9.212	7.425	14.360	
	optB88	2	1.3746	1.3742	60.02	9.491	7.158	13.862	
	Exp. [33]					9.315	6.556	12.804	
					898.8±1.6	632.6±1.5		1235.4±1.5	
Formula: H ₁ N ₁		M			ΔH_f			D_{H+N}	
HN or NH (Imidogen)			l_{HN}						
	PBE	2	1.0506		3.602			3.863	
	optB88	2	1.0485		3.732			4.025	
	AOBM [79]		1.035						
	Exp. [37]		1.0362						
	Exp. [33]				3.7181			3.3981	
					358.74±0.16			327.87±0.16	
Formula: H ₁ N ₁ O ₁		M			ΔH_f	D_{HN+O}	D_{H+NO}	D_{HO+N}	D_{H+N+O}
Linear HNO or ONH			l_{NH}	l_{NO}					
	PBE	2	1.0038	1.2291	2.277	4.349	0.938	3.506	8.212
	optB88	2	1.0022	1.2314	2.440	4.292	1.002	3.431	8.318
Linear HON or NOH			l_{ON}	l_{OH}					

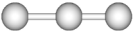

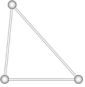
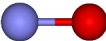
	PBE	2	1.3041	0.9619		3.093	3.533	0.122	2.690	7.396
	optB88	2	1.3097	0.9612		3.201	3.531	0.240	2.669	7.556
Linear OHN or NHO			l_{HN}	l_{HO}						
	PBE	4	2.1373	0.9920		5.750	0.877	-2.534	0.033	4.740
	optB88	4	2.1433	0.9905		5.840	0.893	-2.398	0.031	4.918
Triangular HNO or ONH (Nitrosyl hydride)			l_{NH}	l_{NO}	θ_{HNO}					
	PBE	0	1.0788	1.2168	108.49	0.960	5.666	2.255	4.822	9.529
	optB88	0	1.0757	1.2171	108.57	0.997	5.735	2.445	4.874	9.760
	AOBM	[80]	1.0524	1.2085	108.08					
	Exp.	[81]	1.0628	1.2116	108.058					
	Exp.	[46]	1.09026	1.2090	108.047					
	Exp.	[33]				1.1395	5.1310	2.03894	4.1242	8.5351
					109.94±0.11	495.64±0.19	196.728±0.092	397.92±0.11	823.51±0.11	
Triangular NOH or HON (Hydroxyimidogen)			l_{ON}	l_{OH}	θ_{NOH}					
	PBE	2	1.3341	0.9849	109.04	1.922	4.705	1.294	3.861	8.568
	optB88	2	1.3380	0.9841	109.29	2.041	4.691	1.401	3.829	8.716
	AOBM	[80]	1.3255	0.9676	107.47					
	Exp.	[33]				2.2580	4.0184	0.920	3.0056	7.4166
						217.86±0.77	387.72±0.79	88.81±0.77	290.00±0.77	715.59±0.77
Formula: H_1N_2			M			ΔH_f	$D_{\text{HN+N}}$	$D_{\text{H+N}_2}$	$D_{\text{H+2N}}$	
Linear HNN or NNH			l_{NH}	l_{NN}						
	PBE	1	1.0045	1.1834		3.124	5.674	-0.855		9.538

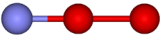
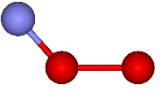
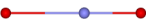
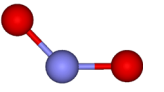
	optB88	1	1.0022	1.1816		3.285	5.711	-0.791	9.736
Linear NHN			l_{HN}	l_{HN}					
	PBE	1	1.0507	2.6013		8.784	0.014	-6.515	3.877
	optB88	1	1.0487	2.5896		8.981	0.015	-6.486	4.040
Triangular HNN or NNH (Diazenyl)			l_{NH}	l_{NN}	θ_{HNN}				
	PBE	1	1.0716	1.1806	118.36	2.016	6.783	0.253	10.646
	optB88	1	1.0698	1.1778	118.42	2.168	6.828	0.326	10.853
	AOBM [82]		1.045	1.157	118.0			0.438-1.184	
	AOBM [83]		1.031-1.060	1.171-1.181	113.2-118.5				
	AOBM [84]		1.062	1.197	116.3			0.323-0.898	
	Exp. [33]					2.6133	5.9821	-0.3743	9.3802
						252.14±0.45	577.18±0.47	-36.11±0.45	905.05±0.45
Formula: H ₁ O ₁			M			ΔH_f			$D_{\text{H+O}}$
OH or HO (Hydroxyl)			l_{HO}						
	PBE	1	0.9868			0.586			4.706
	optB88	1	0.9862			0.607			4.887
	AOBM [85]		0.971						
	AOBM [86]					0.3845			
	Exp. [37]		0.96966						
	Exp. [33]					0.38641			4.41098
						37.283±0.025			425.595±0.024

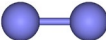
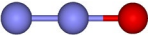
Formula: H ₁ O ₂		<i>M</i>				ΔH_f	$D_{\text{HO}+\text{O}}$	$D_{\text{H}+\text{O}_2}$	$D_{\text{H}+\text{2O}}$
Linear HOO or OOH			l_{OH}	l_{OO}					
	PBE	3	0.9871	5.7400		3.608	0.002	-1.339	4.708
	optB88	3	0.9861	5.7397		3.605	0.002	-1.110	4.889
Linear OHO			l_{HO}	l_{HO}					
	PBE	3	1.1137	1.1195		3.248	0.362	-0.979	5.069
	optB88	3	1.1215	1.1152		3.240	0.367	-0.746	5.253
Triangular HOO (Dioxidanyl)			l_{OH}	l_{OO}	θ_{HOO}				
	PBE	1	0.9902	1.3451	105.01	-0.004	3.614	2.273	8.320
	optB88	1	0.9888	1.3520	104.85	-0.005	3.612	2.499	8.499
	AOBM [87]		1.00	1.35	104				
	AOBM [87]		0.951	1.391	106				
	AOBM [86]					0.1535			
	Exp. [88]		0.9774	1.3339	104.15				
	Exp. [89]		0.9707	1.33054	104.29				
	Exp. [33]					0.1569	2.7879	2.0822	7.1988
						15.14±0.15	268.99±0.15	200.90±0.15	694.58±0.15
Formula: H ₂		<i>M</i>				ΔH_f			
HH (Dihydrogen)			l_{HH}						
	PBE	0	0.7500				0		
	optB88	0	0.7442				0		
	AOBM [90]		0.7668						


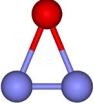

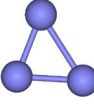
Exp.	[91]		0.74130						
Exp.	[37]		0.74144						
Exp.	[33]								4.478069884 432.0680600 ±0.0000092
<hr/>									
Formula: H_2N_1		M			ΔH_f	$D_{\text{H+HN}}$	$D_{\text{H}_2+\text{N}}$		$D_{2\text{H}+\text{N}}$
Linear NHH or HHN			l_{HN}	l_{HH}					
	PBE	3	2.8632	0.7506	5.189	0.682	0.008		4.546
	optB88	3	2.9003	0.7443	5.259	0.968	0.005		4.993
Linear HNH			l_{NH}	l_{NH}					
	PBE	1	0.9986	0.9986	2.893	2.979	2.304		6.842
	optB88	1	0.9965	0.9965	3.083	3.144	2.180		7.169
Triangular HNH (Amidogen)			l_{NH}	l_{NH}	θ_{HNH}				
	PBE	1	1.0348	1.0347	102.89	1.555	4.317	3.642	8.180
	optB88	1	1.0374	1.0374	102.46	1.739	4.487	3.524	8.512
	AOBM	[92]	1.023	1.023	102.9				
	Exp.	[64]	1.024	1.024	103.4				
	Exp.	[33]				1.9580	3.9991	2.9192	7.3972
						188.92±0.11	385.85±0.17	281.66±0.11	713.72±0.11
<hr/>									
Formula: H_2O_1		M			ΔH_f	$D_{\text{H+HO}}$	$D_{\text{H}_2+\text{O}}$		$D_{2\text{H}+\text{O}}$
Linear OHH or HHO			l_{HO}	l_{HH}					
	PBE	2	0.9922	1.9384	2.833	0.022	0.191		4.729

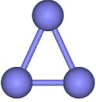
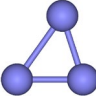

	optB88	2	1.0039	1.5461		3.055	0.047	-0.055	4.934
	Exp. [33]					2.566	0.059	-0.007	4.470
						247.6±2.7	5.7±2.7	-0.7±2.7	431.3±2.7
Linear HOH			l_{OH}	l_{OH}					
	PBE	0	0.9428	0.9428		-1.266	4.122	4.290	8.828
	optB88	0	0.9419	0.9420		-1.182	4.283	4.182	9.170
Triangular1 HOH (Water)			l_{OH}	l_{OH}	θ_{HOH}				
	PBE	0	0.9719	0.9718	104.51	-2.520	5.375	5.544	10.081
	optB88	0	0.9710	0.9709	104.82	-2.433	5.534	5.433	10.421
	AOBM [85]		0.960	0.960	103.4				
	Exp. [93]		0.95781	0.95781	104.4776				
	Exp. [33]					-2.47600	5.101446	5.03436	9.51243
						-238.898±0.025	492.2147±0.0011	485.742±0.024	917.810±0.024
Triangular2 HOH			l_{OH}	l_{OH}	θ_{HOH}				
	PBE	0	2.3306	2.3306	18.66	2.991	-0.136	0.033	4.571
	optB88	0	2.4567	2.4567	17.51	2.982	0.119	0.018	5.006
	Exp. [33]					2.562	0.063	-0.004	4.474
						247.2±2.0	6.1±1.9	-0.4±1.9	431.7±1.9
Formula: H ₃		M				ΔH_f		$D_{\text{H+H}_2}$	$D_{3\text{H}}$
Linear1 HHH			l_{HH}	l_{HH}					
	PBE	0	0.9358	0.9358		3.028	-0.759		3.779
	optB88	0	0.9330	0.9330		3.109	-0.614		4.374


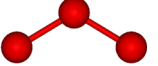
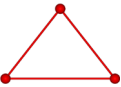
	AOBM	[94]	0.90	0.90				
	AOBM	[95]	0.90-0.95	0.90-0.95				
Linear2 HHH (Trihydrogen)			l_{HH}	l_{HH}				
	PBE	1	0.8877	0.9968	2.428	-0.159	4.379	
	optB88	1	0.8963	0.9773	2.612	-0.118	4.871	
	AOBM	[94]	0.828	1.040				
	AOBM	[95]	0.889	0.995				
	Exp.	[33]			2.638	-0.398	4.079	
					254.5±1.2	-38.4±1.1	393.6±1.1	
Linear3 HHH			l_{HH}	l_{HH}				
	PBE	1	0.7500	4.9214	2.269	0.000	4.538	
	optB88	1	0.7443	4.9213	2.494	0.001	4.989	
	AOBM	[94]	0.74	4.92				
	Exp.	[33]			2.238	0.002	4.479	
					215.9±1.1	0.2±1.1	432.2±1.1	
Triangular (cyclic) HHH			l_{HH}	l_{HH}	θ_{HHH}			
	PBE	3	3.6979	3.8235	83.45	6.805	-4.536	0.002
	optB88	3	4.1644	4.2243	84.30	7.483	-4.988	0.000
Formula: N ₁ O ₁		<i>M</i>			ΔH_f		D_{N+O}	
NO or ON (Nitric oxide)			l_{NO}					
	PBE	1	1.1687		0.946		7.274	
	optB88	1	1.1676		0.948		7.316	

	AOBM	[96]	1.169							
	AOBM	[96]	1.154							
	Exp.	[37]	1.15077							
	Exp.	[33]				0.93940		6.49617		
						90.638±0.066		626.785±0.062		
<hr/>										
Formula: N ₁ O ₂			<i>M</i>		ΔH_f	$D_{\text{NO}+\text{O}}$	$D_{\text{N}+\text{O}_2}$	$D_{\text{N}+\text{2O}}$		
Linear NOO or OON			l_{ON}	l_{OO}						
	PBE	1	1.2215	1.3137	4.623	-0.653	0.574	6.622		
	optB88	1	1.2221	1.3260	4.606	-0.658	0.658	6.657		
Triangular NOO (Peroxyimidogen)										
	PBE	1	1.2019	1.3714	3.389	0.581	1.808	7.855		
	optB88	1	1.1960	1.3948	3.378	0.569	1.885	7.885		
	Exp.	[33]				4.202	-0.704	0.676	5.793	
						405.4±1.9	-67.9±1.9	65.2±1.9	558.9±1.9	
Linear ONO			l_{NO}	l_{NO}						
	PBE	7	3.2516	4.5098	11.228	-7.258	-6.031	0.016		
	optB88	7	3.2515	4.5096	11.247	-7.300	-5.984	0.016		
Triangular ONO (Nitrogen dioxide)			l_{NO}	l_{NO}	θ_{ONO}					
	PBE	1	1.2118	1.2119	133.86	-0.195	4.165	5.391	11.439	
	optB88	1	1.2128	1.2129	133.40	-0.110	4.057	5.373	11.372	
	AOBM	[96]	1.216	1.216	133.7					
	AOBM	[96]	1.202	1.202	134.0					

	Exp.	[64]	1.193	1.193	134.1			
	Exp.	[33]				0.38221	3.1155438	4.49500
						36.878±0.066	300.60428±0.00031	433.702±0.062
Formula: N ₂			<i>M</i>		ΔH_f			<i>D</i> _{2N}
NN (Dinitrogen)			<i>l</i> _{NN}					
	PBE		0	1.1129	0			10.393
	optB88		0	1.1087	0			10.527
	AOBM	[84]		1.102- 1.109				9.19-9.50
	Exp.	[37]		1.09768				
	Exp.	[33]						9.75443
								941.159±0.046
Formula: N ₂ O ₁			<i>M</i>		ΔH_f	<i>D</i> _{N+NO}	<i>D</i> _{N₂+O}	<i>D</i> _{2N+O}
Linear NNO or ONN (Nitrous oxide)			<i>l</i> _{NN}	<i>l</i> _{NO}				
	PBE		0	1.1431	1.1977	0.168	5.974	2.856
	optB88		0	1.1394	1.1996	0.308	5.903	2.692
	AOBM	[97]		1.13	1.21			3.36
	AOBM	[97]		1.12	1.20			3.63
	Exp.	[98]		1.127292	1.185089			
	Exp.	[33]				0.89157	4.9250	1.66678
						86.023±0.096	475.19±0.12	160.820±0.096
								11.4212
								1101.98±0.11
Linear NON			<i>l</i> _{ON}	<i>l</i> _{ON}				
	PBE		0	1.2010	1.2012	4.722	1.420	-1.698
								8.695

	optB88	0	1.2028	1.2027		4.828	1.382	-1.829	8.698
	Exp. [33]					5.654	0.163	-3.096	6.659
						545.5±1.7	15.7±1.7	-298.7±1.7	642.5±1.7
Triangular (cyclic) NON (Oxadiazirene)			l_{ON}	l_{ON}	θ_{NON}				
	PBE	0	1.5344	1.5344	45.98	3.255	2.888	-0.231	10.162
	optB88	0	1.5507	1.5507	45.16	3.294	2.917	-0.294	10.232
	Exp. [33]					3.645	2.171	-1.087	8.668
						351.7±1.7	209.5±1.6	-104.9±1.6	836.3±1.6
Formula: N ₃		M				ΔH_f	$D_{\text{N+N}_2}$		$D_{3\text{N}}$
Linear NNN (Azido radical)			l_{NN}	l_{NN}					
	PBE	1	1.1888	1.1888		3.612	1.584		11.977
	optB88	1	1.1866	1.1866		3.797	1.466		11.993
	AOBM [99]		1.1570	1.1570					
	AOBM [99]		1.1538	1.1538					
	Exp. [100]		1.1815	1.1815					
	Exp. [101]		1.18115	1.18115					
	Exp. [33]					4.6871	0.1901		9.9445
						452.24±0.60	18.34±0.59		959.50±0.5
Triangular1 (cyclic) NNN			l_{NN}	l_{NN}	θ_{NNN}				
	PBE	1	1.3092	1.3092	71.38	5.270	-0.074		10.319
	optB88	1	1.3078	1.3077	72.02	5.521	-0.258		10.269

Triangular2 (cyclic) NNN (1H-Triazirin-1-yl)			l_{NN}	l_{NN}	θ_{NNN}			
	PBE	1	1.4654	1.4654	50.05	5.271	-0.075	10.318
	optB88	1	1.4749	1.4749	49.48	5.509	-0.246	10.281
	B3LYP [102]		1.453	1.453	49.69			
	Exp. [33]					6.07243	-1.195	8.55985
						585.9±2.0	-115.3±1.9	825.9±1.9
Triangular3 (cyclic) NNN			l_{NN}	l_{NN}	θ_{NNN}			
	PBE	1	1.5222	1.3596	70.62	5.271	-0.074	10.319
	optB88	1	1.5381	1.3166	72.01	5.521	-0.258	10.269
Formula: O ₂		M				ΔH_f		D_{20}
OO (Dioxygen)			l_{00}					
	PBE	2	1.2327			0		6.048
	optB88	2	1.2360			0		6.000
	AOBM [96]		1.229					
	AOBM [96]		1.210					
	PBE [103]		1.2343					
	Exp. [104]		1.2074					
	Exp. [37]		1.20752					
	Exp. [33]							5.116708
							493.6873±0.0041	
Formula: O ₃		M				ΔH_f	D_{0+O_2}	D_{30}
Linear OOO			l_{00}	l_{00}				

	PBE	2	1.3098	1.3097	3.778	-0.754	5.294
	optB88	2	1.3176	1.3176	3.688	-0.688	5.312
Triangular OOO (Ozone)			l_{00}	l_{00}	θ_{000}		
	PBE	0	1.2844	1.2840	118.19	1.287	7.784
	optB88	0	1.2894	1.2894	117.99	1.218	7.782
	AOBM	[105]	1.299	1.299	116.0		
	AOBM	[106]	1.277	1.277	116.75		
	AOBM	[96]	1.296	1.296	116.5		
	AOBM	[96]	1.276	1.276	116.9		
	Exp.	[107]	1.278	1.278	116.82		
	Exp.	[108]	1.278	1.278	116.75		
	Exp.	[109]	1.2717	1.2717	116.78		
	Exp.	[110]	1.27276	1.27276	116.7542		
	Exp.	[33]				1.49666	6.1784
						144.406±0.039	596.125±0.039
Triangular (cyclic) OOO			l_{HH}	l_{HH}	θ_{HHH}		
	PBE	6	5.1778	5.1778	76.46	9.067	-6.043
	optB88	6	5.2392	5.2392	75.48	8.999	-5.999

A. Diatomic molecules

The energy of a diatomic molecule is a function of interatomic distance (or atomic spacing), i.e., the potential energy surface (PES) is a one-dimensional (1D) curve. The bond length l between two atoms is defined as the atomic spacing at their equilibrium positions generally corresponding to the sole energy minimum of the PES.

Let us first see 3 one-element diatomic molecules HH or H₂, NN or N₂, and OO or O₂, which are best known in the air in our daily lives. For H₂, the bond lengths 0.7500 Å and 0.7442 Å from our PBE and optB88-vdW calculations reproduce very well the experimental values 0.74144 Å [37] and 0.74130 Å [91]. These values from our PAW DFT calculations are even better than 0.7668 Å from previous Gaussian basis *ab initio* calculations [90]; the dissociation energies 4.458 eV and 4.989 eV from our PBE and optB88-vdW calculations are fairly good when compared with the experimental value 4.4781 eV [33]. For N₂, the bond lengths 1.1129 Å (PBE) and 1.1087 Å (optB88-vdW) also reproduce very well the experimental value 1.09768 Å [37] and very close to the values 1.102 to 1.109 Å from previous AOBM calculations [84]; the dissociation energies 10.393 eV (PBE) and 10.527 eV (optB88-vdW) are fairly good when compared with the experimental value 9.754 eV [33] and the values 9.19 to 9.50 eV from previous AOBM calculations [84]. For O₂, the bond lengths 1.2327 Å (PBE) and 1.2360 Å (optB88-vdW) still reproduce very well the experimental values 1.20752 Å [37] and 1.2074 Å [104], also very close to the values 1.210 to 1.229 Å from previous AOBM calculations [96]; the dissociation energies 6.048 eV (PBE) and 6.000 eV (optB88-vdW) are comparably good with the experimental value 5.117 eV [33].

For the C dimer CC or C₂, the bond lengths 1.3142 Å and 1.3093 Å from our PBE and optB88-vdW calculations somewhat overestimate the experimental value 1.2425 Å [37] than the values 1.247 to 1.255 Å from previous AOBM calculations [65, 66]. As will analyzed below, the errors for C₂ are the upper limits for all bond lengths obtained from our PAW DFT calculations in this work. However, the formation enthalpies 8.780 eV (PBE) and 8.865 eV (optB88-vdW) match well the experimental values 8.499 eV [33] with very low relative errors (see the error analysis in Sec. IV C). The very positive formation enthalpies indicate that forming a C₂ molecule from the bulk graphite is extremely unfavorable. The dissociation energies 6.935 eV (PBE) and 6.704 eV (optB88-vdW) are also comparably good relative to the experimental value 6.248 eV [33] and the AOBM values of 6.072 to 6.371 eV [66]. The very positive dissociation energies indicate that the bond strength in a C₂ molecule is covalently strong.

For CH or HC, the bond lengths 1.1369 Å and 1.1300 Å from our PBE and optB88-vdW calculations have good agreements with the experimental values 1.1199 Å [37] and 1.119786 Å [38], as well as 1.1204 Å from previous AOBM calculation [36]. The formation enthalpies are 6.429 eV (PBE) and 6.384 eV (optB88-vdW), good in line with the experimental value 6.144 eV [33]. The dissociation energies 3.697 eV (PBE) and 3.895 eV (optB88-vdW) are also comparably good relative to the experimental values 3.468 eV [33].

For CN or NC, the bond lengths 1.1768 Å and 1.1733 Å from our PBE and optB88-vdW calculations have excellent agreements with the experimental value 1.1718 Å [37], an AOBM value 1.18 Å [52], and the value 1.162 Å from a hybrid functional B3LYP [53]. The formation enthalpies 4.515 eV (PBE) and 4.606 eV (optB88-vdW) are also in excellent agreements with the experimental value 4.526 eV [33]. The dissociation energies 8.539 eV (PBE) and 8.441 eV (optB88-vdW) are comparable with the experimental value 7.724 eV [33].

For CO or OC, the bond lengths 1.1431 Å and 1.1393 Å from our PBE and optB88-vdW calculations have good agreements with the experimental value 1.128323 Å [37] and the AOBM value 1.1513 Å [62]. Our PBE and optB88-vdW calculations predict the negative formation enthalpies -0.621 eV and -0.715 eV, consistent with the experimental value -1.1795 eV [33]. The negative formation enthalpy indicates that forming CO from gas phase O_2 and bulk graphite is favorable thermodynamically. The dissociation energies 11.502 eV (PBE) and 11.499 eV (optB88-vdW) are in good agreements with the experimental value 11.111 eV [33]. The dissociation energy of CO is largest among those of all 10 diatomic molecules in this section, indicating the strongest bond strength.

For HN or NH, the bond lengths 1.0506 Å and 1.0485 Å from our PBE and optB88-vdW calculations are in good agreements with the experimental value 1.0362 Å [37] and the AOBM value 1.035 Å [79]. The formation enthalpies 3.602 eV (PBE) and 3.732 eV (optB88-vdW) are in excellent agreement with the experimental value 3.718 eV [33]. The dissociation energies 3.863 eV (PBE) and 4.025 eV (optB88-vdW) are fairly good relative to the experimental value 3.398 eV [33].

For HO or OH, the bond lengths 0.9868 Å and 0.9862 Å from our PBE and optB88-vdW calculations are in good agreements with the experimental value 0.96966 Å [37] and the AOBM value 0.971 Å [85]. The formation enthalpies 0.586 eV (PBE) and 0.607 eV (optB88-vdW) are comparable with the experimental value 0.386 eV [33] and the AOBM value 0.3845 eV [86]. The dissociation energies 4.706 eV (PBE) and 4.887 eV (optB88-vdW) are also comparable with the experimental value 4.411 eV [33].

For NO or ON, the bond lengths 1.1687 Å and 1.1676 Å from our PBE and optB88-vdW calculations have good agreements with the experimental value 1.15077 Å [37] and the AOBM values 1.154 Å and 1.169 Å [96]. The formation enthalpies 0.946 eV (PBE) and 0.948 eV (optB88-vdW) are in excellent agreements with the experimental value 0.939 eV [33]. The dissociation energies 7.274 eV (PBE) and 7.316 eV (optB88-vdW) are comparable with the experimental value 6.496 eV [33].

For the above 10 diatomic molecules, we also rank them in order of bond lengths, formation enthalpies, and dissociation energies. From smallest (about 0.74 Å) to largest (about 1.25 Å) bond length, the order from our PBE and optB88-vdW calculations or from experiments is always consistently $HH < HO < HN < NN < CH < CO < NO < CN < OO < CC$. From lowest (about -1 eV) to highest (about 9 eV) formation enthalpy, the order from our PBE and optB88-vdW calculations or from experiments is always consistently $CO < (HH = NN = OO) < HO < NO < HN < CN < CH < CC$, where the formation enthalpy of HH, NN, or OO is zero (i.e., the energy reference point). CO is the sole one with a negative formation enthalpy among the 10 diatomic molecules, indicating that it is most stable thermodynamically relative to its reference systems. From lowest (about 3 eV) to highest (about 11 eV) dissociation energy (i.e., from weakest to strongest bond strength), the order from our optB88-vdW calculations or from experiments is consistently $CH \approx HN < HO < HH < OO < CC < NO < CN < NN < CO$, but there is a switch in the order of HO and HH from our PBE calculations.

B. Triatomic molecules

The energy of a triatomic molecule is a function of three interatomic distances (or equivalently two interatomic distances and the angle between them), and therefore the PES is a 3D curve and much more complicated than the 1D curve for a diatomic molecule. In general, the PES of a triatomic molecule has multiple energy minima corresponding to different structural geometries (or spatial arrangements of atoms) which are commonly called the locally stable isomers, and the global energy minimum corresponds to the most stable isomer. For clarity, we refer to all isomers having the same number of atoms in each element but distinct structural geometries as *one isomer type*. For triatomic molecules consisting of C, H, N, and/or O, there are 20 isomer types in total. In principle, all locally stable isomers of each isomer type can be found by calculating and searching its full 3D PES curve. However, such work is demanding. In this paper, we only focus on several typical isomers for each type, including linear and triangular isomers, especially for those with available data from previous experiments or AOBM calculations.

In Table I, we show the optimized structural geometries of all isomers from our optB88-vdW calculations (the corresponding structural geometries from our PBE calculations are very close to those from the optB88-vdW calculations and therefore not shown). All bond lengths, formation enthalpies, dissociation energies, and spin magnetic moments from our PBE and optB88-vdW calculations, as well as from previous experiments and AOBM calculations, are provided in Table I. In this section, we selectively discuss the 20 types of triatomic molecular isomers. For the isomer types, we adopt the NIST notations [32] for convenient indexing with the formulas in alphabetic order of element symbols and the numbers of elemental atoms in the molecule as subscripts 1, 2, 3, ..., etc. In Table I, the conventional notations and names for isomers are also listed.

For each isomer type, we consider various possible linear and triangular isomers by relaxing the judiciously selected initial configurations, e.g., based on previous experiments or AOBM calculations in the literature. For a linear isomer, the name $\alpha\beta\gamma$ (or equivalently $\gamma\beta\alpha$) indicates that atom β is in the middle position with atoms α and γ on the two sides, where α , β , and γ can be C, H, N, and/or O; correspondingly, the two bond lengths are denoted by $l_{\beta\alpha}$ and $l_{\beta\gamma}$. The triangular isomers can be obtuse (or quasilinear) and acute (or cyclic). The order of atoms in the name of a triangular isomer also indicates the optimized configuration, e.g., for the triangular isomer name $\alpha\beta\gamma$ or $\gamma\beta\alpha$, atom β is in the middle position with atoms α and γ on the two sides; correspondingly, the two bond lengths are denoted by $l_{\beta\alpha}$ and $l_{\beta\gamma}$ with the bond angle denoted as $\theta_{\alpha\beta\gamma}$ or $\theta_{\gamma\beta\alpha}$. Below, we also use notations $\alpha\beta\gamma$ (L), $\alpha\beta\gamma$ (Q), and $\alpha\beta\gamma$ (C) to indicate that the isomer $\alpha\beta\gamma$ is linear, quasilinear triangular, and cyclic triangular, respectively.

$C_1H_1N_1$. We obtain 1 triangular isomer and 3 linear (HCN, HNC, and CHN) isomers. The triangular isomer is cyclic, and no any stable or metastable quasilinear isomer are found. A lower (higher) formation enthalpy indicates a more (less) stable isomer. From more to less stable, the order is HCN (L) > HNC (L) > HCN (C) > CHN (L) with the formation enthalpies of about 1.3 eV, 1.9 eV, 3.3 eV, and 11.6 eV, respectively. Our DFT (PBE and optB88-vdW) values for bond lengths, bond angles,

formation enthalpies, and dissociation energies are in good agreements with available experimental and AOBM values (see Table I). Generally, the experimental measurements for less stable isomers with significantly higher formation enthalpies are often more difficult, and therefore the experimental data for the linear CHN and cyclic isomers are still unavailable in the literature. Note that, for experimental observations, a "less stable" isomer means not only a relatively higher formation enthalpy (i.e., thermodynamically less stable), but also a low energy barrier (i.e., kinetically less stable) from that isomer to another with a lower formation enthalpy, while the latter isomer is "more stable" both thermodynamically and kinetically. In this work, we do not consider the energy barriers between isomers. Therefore, in all statements below, the word "stable" always means "thermodynamically stable", i.e., we omit the word "thermodynamically".

$C_1H_1O_1$. We obtain 2 quasilinear (HCO and HOC) and 3 linear (HCO, HOC, and CHO) isomers. From more to less stable, the order is HCO (Q) > HCO (L) > HOC (Q) > HOC (L) > CHO (L) with the formation enthalpies of about 0.5 eV, 1.5 eV, 1.7 eV, 2.3 eV, and 8.3 eV, respectively. Our DFT values for bond lengths, bond angles, formation enthalpies, and dissociation energies are in good agreements with available experimental and AOBM values for HCO (Q) and HOC (Q) (see Table I). In addition, our DFT values of D_{CO+H} for HOC (L) are zero, indicating no bonding between H and CO, i.e., HOC (L) is not one single "real" molecule but an isolated CO molecule plus an isolated H atom, as also indicated by the large H-O distance beyond 6.6 Å (see Table I). In other words, no energy minimum is found for linear HOC.

C_1H_2 . We obtain 1 quasilinear (HCH) isomer and 2 linear (HCH and CHH) isomers. The most stable isomer is HCH (Q) with the formation enthalpies 3.890 eV (PBE) and 4.176 eV (optB88-vdW), cf. the experimental value 4.053 eV [33]. The C-H bond lengths 1.0849 Å (PBE) and 1.0816 Å (optB88-vdW) as well as the bond angle 135.06° (PBE) and 135.04° (optB88-vdW) are in excellent agreements with the experimental bond length 1.07530 Å of and bond angle of 133.9308° [51] as well as the AOBM bond length 1.07481 Å of and bond angle of 133.839° [50]. In contrast, the isomer HCH (L) is slightly unstable with the formation enthalpies 4.078 eV (PBE) and 4.368 eV (optB88-vdW), while the isomer CHH (L) is extremely unstable with the significantly higher formation enthalpies 7.635 eV (PBE) and 7.704 eV (optB88-vdW). For dissociation energies of HCH (Q), our DFT values are also in good agreements with available experimental values (see Table I).

$C_1N_1O_1$. We obtain 1 triangular isomer and 3 linear (CNO, CON, and NCO) isomers. The triangular isomer is cyclic, and no any stable or metastable quasilinear isomer are found. From more to less stable, the order is NCO (L) > CNO (L) > NCO (C) > CON (L) with the formation enthalpies of about 1 eV, 4 eV, 4.5 eV, and 6 eV, respectively. Our DFT values for bond lengths, bond angles, and formation enthalpies are in good agreements with available experimental and AOBM values (see Table I).

C_1N_2 . We obtain 1 triangular isomer and 2 linear (NCN and CNN) isomers. The triangular isomer is cyclic, and no any stable or metastable quasilinear isomer are found. The most stable isomer is NCN (L) with the formation enthalpies 4.149 eV (PBE) and 4.301 eV (optB88-vdW), cf. the experimental value 4.677 eV [33]. CNN (L) has the formation enthalpies 5.308 eV (PBE) and 5.484 eV (optB88-vdW), while NCN (C) has the highest formation enthalpies 5.733 eV (PBE) and 5.887 eV (optB88-

vdW). Our DFT values for bond lengths and bond angles for these isomers are in good agreements with available B3LYP and AOBM values (see Table I). No experimental data for geometric parameters are available for this isomer type. The difficulty of experimental measurements for these isomers is likely because of their instabilities with the high formation enthalpies beyond 4 eV and likely low energy barriers for dissociations.

C_1O_2 . The most stable isomer from our DFT calculations is linear OCO (L) (i.e., conventionally CO_2) with the very negative formation enthalpies -3.870 eV (PBE) and -3.863 eV (optB88-vdW), cf. the experimental value -4.074 eV [33], indicating its high stability. We also obtain another linear isomer COO (L) and a triangular cyclic isomer, both of which have very positive formation enthalpies and therefore relatively very unstable. For bond length l_{CO} and other formation enthalpies or dissociation energies, our DFT values are also comparably good relative to available experimental and AOBM values (see Table I).

C_2H_1 . The most stable isomer from our DFT calculations is linear CCH (L) with the very positive formation enthalpies 5.938 eV (PBE) and 6.175 eV (optB88-vdW), cf. the experimental value 5.843 eV [33], indicating its high instability. For bond lengths l_{CC} and l_{CH} , as well as dissociation energies of CCH (L), our DFT values have good agreements with available experimental and AOBM values (see Table I). A triangular cyclic isomer is obtained with the higher formation enthalpies 6.750 eV (PBE) and 7.016 eV (optB88-vdW). We also obtain another linear isomer CHC (L) with very high formation enthalpies 12.903 eV (PBE) and 13.054 eV (optB88-vdW).

C_2N_1 . The most stable isomer from our DFT calculations is linear CNC (L) with the very positive formation enthalpies 6.873 eV (PBE) and 6.892 eV (optB88-vdW), cf. the experimental value 6.967 eV [33], indicating its high instability. We also obtain another linear isomer CCN (L) with slightly higher formation enthalpies 6.929 eV (PBE) and 6.966 eV (optB88-vdW). The high instability makes experimental measurements difficult for its structural parameters [71]. A triangular cyclic isomer is also obtained with the further higher formation enthalpies 7.375 eV (PBE) and 7.531 eV (optB88-vdW). For bond lengths, formation enthalpies, and dissociation energies of all these isomers, our DFT values have good agreements with available experimental and AOBM values (see Table I).

C_2O_1 . The most stable isomer from our DFT calculations is linear CCO (L) with the formation enthalpies 3.876 eV (PBE) and 3.991 eV (optB88-vdW), cf. the experimental values 3.909 eV [33]. For bond lengths l_{CC} and l_{CO} , as well as dissociation energies, our DFT values are comparably good relative to available experimental and AOBM values (see Table I). A triangular isomer CCO (Q) with bond angles 109.034° (PBE) and 108.665° (optB88-vdW) (see Table I) is obtained with the much higher formation enthalpies 5.957 eV (PBE) and 6.008 eV (optB88-vdW). We also obtain another linear isomer COC (L) with high formation enthalpies 6.501 eV (PBE) and 6.575 eV (optB88-vdW). The formation enthalpies and dissociation energies of these isomers are also in good agreements with the experimental values listed in Table I.

C₃. Our DFT results show that the PES from quasilinear CCC (Q) to linear CCC (L) is almost flat in the region with the bond angles close to 180°. From our PBE calculations, the change in formation enthalpy is only 0.0058 eV (from 8.6997 eV to 8.7055 eV) with the bond length from 1.3027 Å to 1.3018 Å and the bond angle from 149.255° to 180°. From our optB88-vdW calculations, the change in formation enthalpy is only -0.0002 eV (from 8.6579 eV to 8.6577 eV) with the bond length from 1.2949 Å to 1.2948 Å and the bond angle from 170.243° to 180°. This energy degenerate behavior from CCC (Q) to linear CCC (L) is consistent with previous AOBM calculations [78, 111]. These DFT bond lengths, formation enthalpies, and dissociation energies are in good agreements with previous experimental and AOBM data (see Table I). We also obtain a cyclic isomer CCC (C) with formation enthalpies 9.212 eV (PBE) and 9.491 eV (optB88-vdW) which are higher (i.e., the isomer is less stable) than the above values for CCC (Q) or CCC (L). Also note that the spin magnetic momentum $M = 2 \mu_B$ of CCC (C) is different from $M = 0 \mu_B$ for CCC (Q) or CCC (L). Note that the formation enthalpy and dissociation energies for the cyclic isomer are also in good agreements with the experimental values in Table I.

H₁N₁O₁. We obtain 2 quasilinear (HNO and HON) and 3 linear (HNO, HON, and NHO) isomers. From more to less stable, the order is HNO (Q) > HON (Q) > HNO (L) > HON (L) > NHO (L) with the formation enthalpies of about 1.0 eV, 2.0 eV, 2.4 eV, 3.2 eV, and 5.8 eV, respectively. The bond lengths, bond angles, formation enthalpies, and dissociation energies from our DFT calculations are in good agreements with available experimental and AOBM values (see Table I).

H₁N₂. The most stable isomer from our DFT calculations is quasilinear HNN (Q) with the formation enthalpies 2.016 eV (PBE) and 2.168 eV (optB88-vdW), cf. the experimental value 2.613 eV [33]. The values 0.253 eV (PBE) and 0.326 eV (optB88-vdW) for dissociation energy D_{H+N_2} of HNN(Q) are comparable to the AOBM values 0.438 eV to 1.184 eV [82] and 0.323 eV to 0.898 eV [84], cf. the relatively slightly negative value -0.374 eV from experiments [33]. Other PBE and optB88-vdW dissociation energies are also comparable with the experimental values in Table I. The bond lengths and bond angles from our DFT calculations are in good agreements with available AOBM values (see Table I), while the experimental data in the literature are unavailable for these geometric parameters. We also obtain the linear isomer HNN (L) with higher formation enthalpies 3.124 eV (PBE) and 3.285 eV (optB88-vdW), as well as the linear isomer NHN (L) with much higher formation enthalpies 8.784 eV (PBE) and 8.981 eV (optB88-vdW). In addition, our DFT values of D_{HN+N} for NHN (L) are 0.014 eV (PBE) and 0.015 eV (optB88-vdW), indicating a weak bond between N and HN with the bond length of about 2.6 Å (see Table I), which approaches the range of vdW interactions.

H₁O₂. The most stable isomer from our DFT calculations is triangular HOO (Q) with the slightly negative formation enthalpies -0.004 eV (PBE) and -0.005 eV (optB88-vdW), cf. the positive but relatively low experimental value 0.157 eV [33] and AOBM value 0.1535 eV [86]. All dissociation energies from PBE and optB88-vdW calculations for HOO(Q) are comparable to the experimental values [33] in Table I. The bond lengths and bond angles from our DFT calculations are in good agreements with available experimental values (also see Table I). For the linear isomer HOO (L), we obtain the significantly

higher formation enthalpies 3.608 eV (PBE) and 3.605 eV (optB88-vdW), as well as $D_{\text{HO}+\text{O}} = 0.002$ eV (PBE and optb88-vdW), indicating negligible bonding between O and HO, i.e., they are almost isolated, as indicated by the large O-O distance beyond 5.7 Å (see Table I). In addition, we also obtain the linear isomer OHO (L) with formation enthalpies 3.248 eV (PBE) and 3.240 eV (optB88-vdW).

H_2N_1 . The most stable isomer from our DFT calculations is triangular HNH (Q) with the formation enthalpies 1.555 eV (PBE) and 1.739 eV (optB88-vdW), cf. the experimental value 1.958 eV [33]. All dissociation energies from PBE and optB88-vdW calculations for HNH(Q) are comparable to the experimental values [33] in Table I. The bond lengths and bond angles from our DFT calculations for HNH (Q) are in good agreements with available experimental and AOBM values (also see Table I). We also obtain the linear isomer HNH (L) with significantly higher formation enthalpies 2.893 eV (PBE) and 3.083 eV (optB88-vdW). For the linear isomer HHN (L), we obtain further significantly higher formation enthalpies 5.189 eV (PBE) and 5.259 eV (optB88-vdW), as well as $D_{\text{H}_2+\text{N}} = 0.008$ eV (PBE) and 0.005 eV (optb88-vdW), indicating negligible bonding between N and HH, i.e., both N and HH (or H_2) are nearly isolated, as indicated by the large H-N distance beyond 2.8 Å (see Table I again).

H_2O_1 . The most stable isomer from our DFT calculations is triangular HOH (Q) with the negative formation enthalpies -2.520 eV (PBE) and -2.433 eV (optB88-vdW) which match well the experimental value -2.476 eV [33]. The bond lengths and bond angles from our DFT calculations for HOH (Q) are in excellent agreements with available experimental and AOBM values (see Table I). We also obtain a triangular HOH, which is actually a complex with weak vdW interaction between O and HH, as indicated by $D_{\text{H}+\text{HO}} \approx 0$ (see Triangular2 HOH in Table I). For the linear isomer OHH (L), we obtain positive formation enthalpies 2.833 eV (PBE) and 3.055 eV (optB88-vdW), as well as $D_{\text{H}+\text{HO}} = 0.022$ eV (PBE) and 0.047 eV (optb88-vdW), again indicating weak bonding between H and HO. The formation enthalpies and dissociation energies from the DFT calculations for these isomers have good consistency with the experimental values in Table I. Additionally, we also obtain the linear isomer HOH (L) with higher but still negative formation enthalpies -1.266 eV (PBE) and -1.182 eV (optB88-vdW).

H_3 . The PES of linear HHH are available from the early ABOM work [94, 95]. From the PES, there are no stable linear geometries for 3 bonded H atoms. To assess the consistency of our DFT results with these ABOM results, we first select 2 locally equilibrium linear HHH with short bond lengths around 1 Å (see linear1 and linear2 HHH in Table I) and always obtain the negative $D_{\text{H}+\text{H}_2}$, which indeed indicates the instabilities of these two linear geometries. We also obtain a linear geometry with two H-H distances of about 0.75 Å and 4.72 Å (see linear3 HHH in Table I) and lowest formation enthalpies 2.269 eV (PBE) and 2.494 eV (optB88-vdW), as well as $D_{\text{H}+\text{H}_2} = 0.000$ eV (PBE) and 0.001 eV (optb88-vdW), indicating no bonding between H and HH, i.e., a system of an isolated H atom plus an isolated H_2 molecule is more stable than any linearly fully bonded HHH. For the consistency of formation enthalpies and other dissociation energies of these isomers from the DFT calculations with available experimental data, see Table I. In early work [112, 113, 114], equilateral triangular states with the

side lengths of about 0.85 Å for HHH are predicted. However, we cannot find such fully bonded triangular HHH from our DFT calculations. Instead, we find that three H atoms for any initially triangular HHH always become isolated after full relaxation (see, e.g., a triangular cyclic HHH in Table I), as indicated by the corresponding $D_{3\text{H}} = 0.002$ eV (PBE) and 0.000 eV (optb88-vdW). This seems to imply that the fully bonded stable H_3 structures do not exist at all, thus consistent with our above DFT predictions. This instability is also consistent with the very negative experimental values of $D_{\text{H}+\text{H}_2} = -5.491$ eV and $D_{3\text{H}} = -1.013$ eV [33] for an equilateral triangular state.

N_1O_2 . The most stable isomer from our DFT calculations is triangular ONO (Q) (i.e., conventionally NO_2) with the negative formation enthalpies -0.195 eV (PBE) and -0.110 eV (optB88-vdW), cf. the positive but quite low experimental value 0.382 eV [33]. For bond length l_{NO} and bond angle θ_{ONO} , our DFT values are in excellent agreements with available experimental and AOBM values (see Table I). The dissociation energies from the DFT calculations are comparable with the experimental values (see Table I). For the linear isomer ONO (L), we obtain much higher DFT formation enthalpies of about 11.2 eV, as well as $D_{\text{N}+\text{O}} = 0.016$ eV, indicating weak bonding between three atoms with large bond lengths beyond 3.2 Å. We also obtain the linear isomer NOO (L) with DFT formation enthalpies of about 4.6 eV. Again, the relatively high formation enthalpies imply high instabilities of the linear isomers. We also obtain a triangular NOO (Q) (see Table I) with a relatively small positive $D_{\text{NO}+\text{O}} \approx 0.6$ eV, indicating weak bonding between O and NO, while the corresponding experimental value -0.704 eV [33] is slightly negative, indicating the instability of this isomer. We also tried to obtain a cyclic ONO, but no stable configuration was found. This is also consistent with the negative value of $D_{\text{NO}+\text{O}} \approx -0.182$ eV (again indicating the instability of the isomer) from experiments [33].

N_2O_1 . The most stable isomer from our DFT calculations is linear NNO (L) with the formation enthalpies 0.168 eV (PBE) and 0.308 eV (optB88-vdW), cf. the experimental value 0.892 eV [33]. The bond lengths from our DFT calculations are in excellent agreements with available experimental and AOBM values (see Table I). For the linear isomer NON (L), we obtain much higher DFT formation enthalpies of about 4.8 eV. We also obtain an isosceles triangular isomer NON (C) with DFT formation enthalpies of about 3.3 eV (see triangular cyclic NON in Table I). Both NON (L) and NON (C) have the relatively high formation enthalpies implying their instabilities relative to NNO (L). For the dissociation energies of these isomers, the DFT values also have good agreements with the experimental values and AOBM values, as listed in Table I.

N_3 . The most stable isomer from our DFT calculations is the linearly symmetric NNN (L) with the formation enthalpies 3.612 eV (PBE) and 3.797 eV (optB88-vdW), cf. the experimental value 4.687 eV [33]. The bond lengths 1.1888 Å (PBE) and 1.1866 Å (optB88-vdW) from our DFT calculations are in excellent agreements with the experimental values 1.1815 Å [100] and 1.18115 Å [101], even better than the AOBM values 1.1570 Å and 1.1538 Å [99]. We also obtain three triangular isomers with slightly different geometries (see triangular1, triangular2, triangular3 for cyclic NNN in Table I) and formation enthalpies (about 5.5 eV). For the triangular2, the bond lengths and bond angle are consistent with the previous B3LYP values [102], as

well as the formation enthalpies with experimental values (see again triangular₂ for cyclic NNN in Table I). For the consistency of dissociation energies between the DFT and experimental values, see Table I.

O₃. The most stable isomer from our DFT calculations is quasilinear OOO (Q) with the formation enthalpies 1.287 eV (PBE) and 1.218 eV (optB88-vdW), cf. the experimental value 1.497 eV [33]. The bond lengths from our DFT calculations are in good agreements with available experimental and AOBM values (see Table I). The dissociation energy D_{O+O_2} values of OOO (Q) are 1.737 eV (PBE) and 1.782 eV (optB88-vdW), cf., the experimental value 1.06 eV [33]. The dissociation energy D_{3O} values of OOO (Q) are 7.784 eV (PBE) and 7.782 eV (optB88-vdW), cf., the experimental value 6.178 eV [33]. For the linear isomer OOO (L), we obtain higher DFT formation enthalpies of about 3.7 eV, and thus it is relatively unstable. We also try to calculate cyclic geometries and obtain a configuration with 3 almost isolated O atoms (see triangular cyclic OOO in Table I), for which the formation enthalpies are about 9 eV high and the D_{3O} values are nearly zero, implying no stable bonded cyclic OOO isomers. This is also consistent with a negative value of $D_{O+O_2} = -0.268$ eV from experiments for a cyclic OOO isomer [33].

C. NO₃ and HNO₃ molecules

As described in Sec. III B, the PES of a triatomic molecule can be much more complicated than the 1D curve for a diatomic molecule. A PES for a 4-atom (e.g., NO₃) or 5-atom (e.g., HNO₃) molecule will be even more complicated, and therefore obtaining the full PES with all spatial arrangements of atoms is impractical computationally. In this section, we choose the initial configurations based on previous experiments and perform our DFT structure optimizations for NO₃ and HNO₃ molecules.

1. NO₃

From experiments [115], the NO₃ has a planar structure of D_{3h} symmetry (see Table II) in the ground electronic state. It is interesting to first note that there is a long dispute on the symmetry breaking of NO₃ from various quantum chemical investigations [116, 117, 118, 119] (also see more references cited in Ref. [124]), until Eisfeld *et al.* use the CASSCF approach (which is an AOBM) to recognize that the C_{2v} geometry previously obtained from different AOBM calculations is likely artificially erroneous [119, 120]. Thus, it is very necessary and interesting to examine the geometric symmetry of a NO₃ molecule from the PAW DFT method.

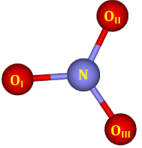
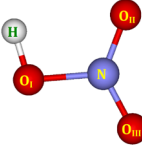
As listed in Table II, the optimized geometry of NO₃ from our DFT calculations is of D_{3h} symmetry and no stable C_{2v} geometry is found, therefore consistent with experiments and the above CASSCF calculations from Eisfeld *et al.* The bond lengths 1.251 Å (PBE) and 1.252 Å (optB88-vdW) are in good agreements with the experimental value 1.240 Å [115], as well as previous ABOM values 1.2518 Å [119], 1.24 Å [121], and 1.246 Å [122].

The formation enthalpies -0.213 eV (PBE) and -0.136 eV (optB88-vdW) are negative, in contrast to the positive experimental value 0.823 eV [33]. The dissociation energy $D_{\text{NO}_2+\text{O}}$ values 3.042 eV (PBE) and 3.027 eV (optB88-vdW) are comparable to the experimental value 2.118 eV [33]. For a comparison of other dissociation energies, see Table II. For the error analysis and discussion relevant to these data, see Sec. IV C.

2. HNO₃

By fully relaxing different initial geometries, e.g., based on three planar (2D) models and one 3D model assumed by Maxwell *et al.* [123], the most stable configuration for a HNO₃ molecule is a planar structure from our DFT calculations, e.g., the optimized geometry from our optB88-vdW calculations is shown in Table II. All bond lengths and bond angles from our PBE and optB88-vdW calculations are in excellent agreements with previous experimental data [123, 124] and AOBM values [125] (see Table II). The formation enthalpies -2.107 eV (PBE) and -2.005 eV (optB88-vdW) are negative, in good agreements with the experimental value -1.290 eV [33]. Again, for a comparison of other dissociation energies, see Table II; for the error analysis and discussion relevant to these data, see Sec. IV C.

TABLE II. Theoretical and experimental data for NO_3 and HNO_3 molecules. For the notation details, see the caption of Table I.

Formula: N_1O_3		M			ΔH_f	$D_{\text{NO}_2+\text{O}}$	$D_{\text{NO}+\text{O}_2}$	$D_{3\text{O}+\text{N}}$
Planar NO_3 (nitrogen trioxide, etc.)			$l_{\text{NO}_1} = l_{\text{NO}_{\text{II}}} = l_{\text{NO}_{\text{III}}}$	$\theta_{\text{O}_1\text{NO}_{\text{II}}} = \theta_{\text{O}_{\text{II}}\text{NO}_{\text{III}}} = \theta_{\text{O}_{\text{III}}\text{NO}_1}$				
	PBE	1	1.251	120.0	-0.213	3.042	1.159	14.481
	optB88	1	1.252	120.0	-0.136	3.027	1.084	14.399
	AOBM	[121]	1.24	120				
	AOBM	[122]	1.246	120				
	AOBM	[119]	1.2518	120				
	Exp.	[115]	1.240	120				
	Exp.	[33]				0.8229	2.1176	0.1165
					79.40±0.19	204.32±0.17	11.24±0.17	1131.71±0.18
Formula: $\text{H}_1\text{N}_1\text{O}_3$		M			ΔH_f	$D_{\text{H}+\text{NO}_3}$	$D_{\text{HO}+\text{NO}_2}$	$D_{\text{H}+\text{N}+3\text{O}}$
Planar HNO_3 (nitric acid, etc.)								
	PBE	0	$l_{\text{NO}_1} = 1.44571$ $l_{\text{NO}_{\text{II}}} = 1.22310$ $l_{\text{NO}_{\text{III}}} = 1.20878$ $l_{\text{HO}_1} = 0.98328$	$\theta_{\text{O}_1\text{NO}_{\text{II}}} = 115.4725$ $\theta_{\text{O}_1\text{NO}_{\text{III}}} = 113.5584$ $\theta_{\text{O}_{\text{II}}\text{NO}_{\text{III}}} = 130.9692$ $\theta_{\text{HO}_1\text{N}} = 101.9683$	-2.107	4.163	2.498	18.644
	optB88	0	$l_{\text{NO}_1} = 1.45489$ $l_{\text{NO}_{\text{II}}} = 1.22329$ $l_{\text{NO}_{\text{III}}} = 1.20875$ $l_{\text{HO}_1} = 0.98258$	$\theta_{\text{O}_1\text{NO}_{\text{II}}} = 115.4328$ $\theta_{\text{O}_1\text{NO}_{\text{III}}} = 113.4929$ $\theta_{\text{O}_{\text{II}}\text{NO}_{\text{III}}} = 131.0743$ $\theta_{\text{HO}_1\text{N}} = 102.0232$	-2.005	4.363	2.502	18.762
	AOBM	[125]	$l_{\text{NO}_1} = 1.39960$	$\theta_{\text{O}_1\text{NO}_{\text{II}}} = 115.7199$				

		$l_{\text{NO}_{\text{II}}} = 1.21032$	$\theta_{\text{O}_1\text{NO}_{\text{III}}} = 114.0088$		
		$l_{\text{NO}_{\text{III}}} = 1.19531$	$\theta_{\text{O}_{\text{II}}\text{NO}_{\text{III}}} = 130.2713$		
		$l_{\text{HO}_1} = 0.96985$	$\theta_{\text{HO}_1\text{N}} = 102.2040$		
Exp.	[123]	$l_{\text{NO}_1} = 1.41 \pm 0.02$	$\theta_{\text{O}_1\text{NO}_{\text{II}}} = 115 \pm 2.5$		
		$l_{\text{NO}_{\text{II}}} = 1.22 \pm 0.02$	$\theta_{\text{O}_1\text{NO}_{\text{III}}} = 115 \pm 2.5$		
		$l_{\text{NO}_{\text{III}}} = 1.22 \pm 0.02$	$\theta_{\text{O}_{\text{II}}\text{NO}_{\text{III}}} = 130 \pm 5$		
Exp.	[124]	$l_{\text{NO}_1} = 1.406$	$\theta_{\text{O}_1\text{NO}_{\text{II}}} = 115.88$		
		$l_{\text{NO}_{\text{II}}} = 1.211$	$\theta_{\text{O}_1\text{NO}_{\text{III}}} = 113.85$		
		$l_{\text{NO}_{\text{III}}} = 1.199$	$\theta_{\text{O}_{\text{II}}\text{NO}_{\text{III}}} = 130.27$		
		$l_{\text{HO}_1} = 0.964$	$\theta_{\text{HO}_1\text{N}} = 102.15$		
Exp.	[33]			-1.2900	4.3520
				-124.47±0.18	419.90±0.23
					2.0587
					16.0813
					198.63±0.17
					1551.61±0.17

IV. Error analysis relative to experimental data

To assess the reliability of a DFT method by rating the quality or accuracy of the obtained DFT values, the corresponding error analysis is always needed. Before performing error analysis, it is necessary to make a review for the definitions of the errors often used for rating DFT values in the literature. For the i th value Q_i in a dataset of DFT values from $i = 1$ to n (where n is often called the sample size), the absolute error (AE) is defined as

$$\Delta Q_i \equiv Q_i - Q_{0i}, \quad (1)$$

where the reference Q_{0i} is often taken to be the corresponding experimental value. The quantity “ Q ” can be, e.g., bond length l , bond angle θ , formation enthalpy ΔH_f , or dissociation energy $D_{p_1+p_2+p_3+\dots}$. In this work, we always select the appropriate experimental data as the reference values Q_{0i} . Then, $\Delta Q_i > 0$ indicates overestimation of the experimental value and $\Delta Q_i < 0$ indicates underestimation. The mean absolute error (MAE) over the n DFT values is defined as

$$\Delta Q_{\text{MAE}} \equiv \frac{1}{n} \sum_{i=1}^n |\Delta Q_i|, \quad (2)$$

which describes the mean deviation in the magnitudes of DFT values. Note that the mean error (ME)

$$\Delta Q_{\text{ME}} \equiv \frac{1}{n} \sum_{i=1}^n \Delta Q_i \quad (3)$$

is generally not very appropriate for assessing DFT values because of the cancellation in positive and negative ΔQ_i values, although ME values are often given in the literature.

The relative error (RE) or percentage error (PE) is defined as

$$\delta Q_i \equiv \frac{Q_i - Q_{0i}}{Q_{0i}} \times 100\%. \quad (4)$$

The mean absolute relative error (MARE) or mean absolute percentage error (MAPE) is defined as

$$\delta Q_{\text{MAPE}} \equiv \frac{1}{n} \sum_{i=1}^n |\delta Q_i|, \quad (5)$$

and the mean relative error (MRE) or mean percentage error (MPE) is defined as

$$\delta Q_{\text{MPE}} \equiv \frac{1}{n} \sum_{i=1}^n \delta Q_i. \quad (6)$$

Here, we need to mention that in the literature, the RE (or PE), MARE (or MAPE), and MRE (or MPE) are often given to assess DFT values, but sometimes using these errors is not very instructive (even misleading) especially for relatively small magnitudes, e.g., for the magnitudes ($\lesssim 0.2$ eV) of atomization energies of inert gas crystals [126], which are very sensitive to their AEs, as will be mentioned below.

For the above dataset $\{Q_i\}$, we also give the corresponding standard deviation

$$s = \sqrt{\frac{1}{n} \sum_{i=1}^n |\Delta Q_i|^2} \text{ or } s = \sqrt{\frac{1}{n} \sum_{i=1}^n |\delta Q_i|^2}. \quad (7)$$

Note that the standard deviation s reflects the discreteness of the dataset $\{|\Delta Q_i|\}$ or $\{|\delta Q_i|\}$. Larger (smaller) s indicates that the dataset is more (less) discrete.

It must be mentioned that a quantity often has a significant uncertainty from different experimental measurements. In Tables I and II, the experimental data for formation enthalpies and dissociation energies from ATcT are listed with uncertainties corresponding to estimated 95% confidence limits [34, 35]. To describe the uncertainty for a dataset $\{Q_i\}$, one can also give a corresponding confidence limit by

$$u_{1-\alpha} = \pm t_{\alpha,n} s, \quad (8)$$

where s is obtained from Eq. (7) and $t_{\alpha,n}$ with the confidence level $1 - \alpha$ is an n -dependent factor related to Student's t -distribution. For a 95% confidence interval, α in Eq. (8) is equal to $1 - 0.95 = 0.05$ and then $t_{\alpha,n}$ can be determined from the degree of freedom n . The 95% confidence limit described by Eq. (8) gives an estimate of what kind of accuracy could be expected when the same kind of quantity (e.g., the formation enthalpy) for an additional molecule or isomer (not contained in the dataset $\{Q_i\}$) is calculated. It should be noted that Eq. (8) has a different form from the well-known confidence intervals for evaluating the uncertainty of a new measurement after n measurements of a quantity for a given molecule.

In the error analysis below, the selected reference experimental values based on Tables I and II for bond lengths, bond angles, formation enthalpies, and dissociation energies are provided in Tables S1, S2, S3, and S4 in the supplementary material, respectively. In the selection of experimental data for formation enthalpies or dissociation energies, we have considered the datasets used previously in assessment of PBE GGA [127, 128, 129, 130, 131, 132, 133, 134, 135]. Fortunately, the recently updated ATcT values [33] have been already available for most of formation enthalpies and dissociation energies of molecules or isomers in this work and therefore the ATcT values are prioritized, as listed in Tables I and II, as well as in Tables S3 and S4 with more significant figures.

A. Bond lengths

By selecting 42 bond lengths based on the available experimental data in Tables I and II, the AEs (Δl) and PEs (δl) of the corresponding PBE and optB88-vdW values are plotted in Fig. 1. Among these bond lengths, the AE or $|\text{AE}|$ maxima are $\Delta l_{\max} = |\Delta l|_{\max} = 0.072 \text{ \AA}$ (PBE) and 0.067 \AA (optB88-vdW) for l_{CC} of CC or C₂ dimer. The AE minima are $\Delta l_{\min} = -0.013 \text{ \AA}$ (PBE) for l_{CO} of linear NCO and -0.015 \AA (optB88-vdW) for l_{NH} of triangular HNO. The $|\text{AE}|$ minima are $|\Delta l|_{\min} = 0.005 \text{ \AA}$ (PBE) for l_{CN} of CN and 0.000 \AA (optB88-vdW) for l_{CC} of linear CCC or C₃ trimer.

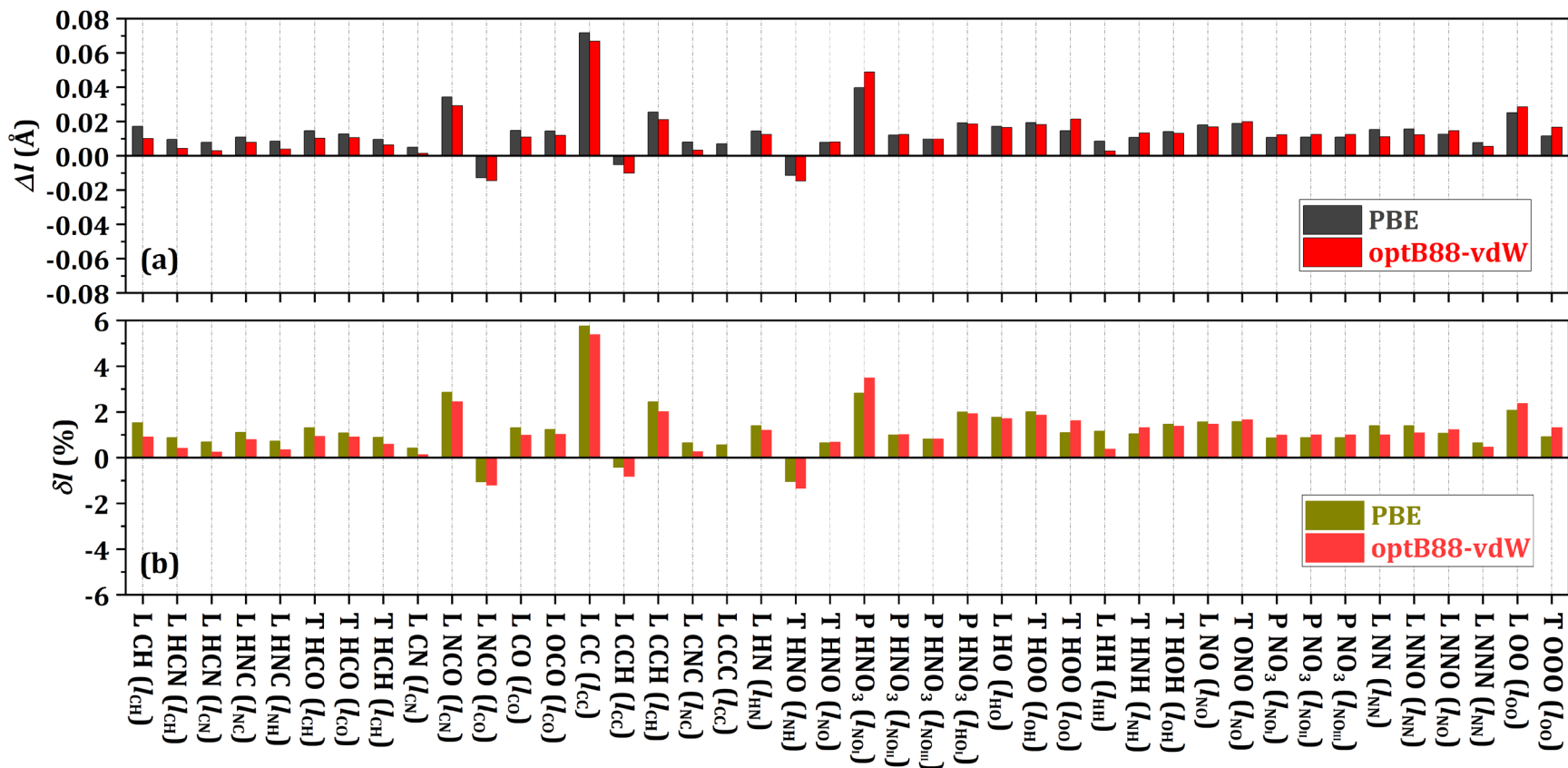


FIG. 1. (a) AEs and (b) PEs of 42 bond lengths. On the horizontal axis, “L” denotes “linear”, “T” denotes “triangular”, and “P” denotes “planar”. For original data, see Table S1.

The PE or $|PE|$ maxima are $\delta l_{\max} = |\delta l|_{\max} = 5.768\%$ (PBE) and 5.374% (optB88-vdW) for l_{CC} of CC or C₂ dimer. The PE minima are $\delta l_{\min} = -1.061\%$ (PBE) for l_{CO} of linear NCO and -1.339% (optB88-vdW) for l_{NH} of triangular HNO. The $|PE|$ minima are $|\delta l|_{\min} = 0.427\%$ (PBE) for l_{CN} of CN and 0.005% (optB88-vdW) for l_{CC} of linear CCC or C₃ trimer.

The MAEs (as well as the standard deviations and uncertainties) of these 42 bond lengths are $\Delta l_{MAE} = 0.015$ ($s = 0.019, u_{0.95} = \pm 0.038$) Å (PBE) and 0.014 ($s = 0.019, u_{0.95} = \pm 0.037$) Å (optB88-vdW). Correspondingly, the MAPEs (as well

as s and $u_{0.95}$ values) are $\delta l_{\text{MAPE}} = 1.345\%$ ($s = 1.616\%$, $u_{0.95} = \pm 3.262\%$) (PBE) and 1.228% ($s = 1.542\%$, $u_{0.95} = \pm 3.111\%$) (optB88-vdW). All above errors are also summarized in Table III.

For comparison, below we list the MAEs and MAPEs (as well as s and $u_{0.95}$ values) for equilibrium lattice constants of solids or equilibrium bond lengths of molecules from similar or different PBE or optB88-vdW calculations in the literature. The s and $u_{0.95}$ values are obtained by using the original data in these references.

$\Delta l_{\text{MAE}} = 0.060$ ($s = 0.069$, $u_{0.95} = \pm 0.145$) Å and $\delta l_{\text{MAPE}} = 1.297\%$ ($s = 1.458\%$, $u_{0.95} = \pm 3.063\%$) for equilibrium lattice constants of 18 tested solids from the planewave PBE calculations of Wu *et al.* [130].

$\Delta l_{\text{MAE}} = 0.071$ ($s = 0.084$, $u_{0.95} = \pm 0.172$) Å and $\delta l_{\text{MAPE}} = 1.411\%$ ($s = 1.591\%$, $u_{0.95} = \pm 3.248\%$) for equilibrium lattice constants of 30 tested solids from the PAW PBE calculations of Schimka *et al.* [131].

$\Delta l_{\text{MAE}} = 0.067$ ($s = 0.079$, $u_{0.95} = \pm 0.163$) Å and $\delta l_{\text{MAPE}} = 1.403\%$ ($s = 1.614\%$, $u_{0.95} = \pm 3.338\%$) for equilibrium lattice constants of 23 tested solids from the PAW PBE calculations of Klimeš *et al.* [132].

$\Delta l_{\text{MAE}} = 0.066$ ($s = 0.074$, $u_{0.95} = \pm 0.154$) Å and $\delta l_{\text{MAPE}} = 1.361\%$ ($s = 1.460\%$, $u_{0.95} = \pm 3.020\%$) for equilibrium lattice constants of 23 tested solids from the PAW optB88-vdW calculations of Klimeš *et al.* [132].

$\Delta l_{\text{MAE}} = 0.037$ ($s = 0.059$, $u_{0.95} = \pm 0.122$) Å and $\delta l_{\text{MAPE}} = 1.367\%$ ($s = 2.278\%$, $u_{0.95} = \pm 4.674\%$) for shortest interatomic distances of 27 transition metals from the PAW PBE calculations of Janthon *et al.* [133].

$\Delta l_{\text{MAE}} = 0.061$ ($s = 0.075$, $u_{0.95} = \pm 0.151$) Å and $\delta l_{\text{MAPE}} = 1.246\%$ ($s = 1.448\%$, $u_{0.95} = \pm 2.919\%$) for equilibrium lattice constants of 44 tested solids from the PBE calculations of Tran *et al.* by using the augmented planewave plus local orbitals (APW+lo) method [16].

$\Delta l_{\text{MAE}} = 0.062$ ($s = 0.075$, $u_{0.95} = \pm 0.151$) Å and $\delta l_{\text{MAPE}} = 1.252\%$ ($s = 1.418\%$, $u_{0.95} = \pm 2.857\%$) for equilibrium lattice constants of 44 tested solids from the APW+lo optB88-vdW calculations of Tran *et al.* [16].

From the above list, the PAW PBE or optB88-vdW results of 42 bond lengths from our DFT calculations are highly satisfactory with a smaller MAE (as well as smaller s and $u_{0.95}$ values) and a similar MAPE relative to the values for solids from various PBE or optB88-vdW calculations in the literature.

In addition, based on the data for equilibrium bond lengths of 16 dimers from the PAW PBE calculations of Paier *et al.* [134], $\Delta l_{\text{MAE}} = 0.013$ ($s = 0.018$, $u_{0.95} = \pm 0.038$) Å and $\delta l_{\text{MAPE}} = 0.832\%$ ($s = 0.992\%$, $u_{0.95} = \pm 2.103\%$), which are very close to the MAE and MAPE values (as well as the corresponding s and $u_{0.95}$ values) for the above 42 bond lengths from our PAW PBE or optB88-vdW calculations. Based on the data for equilibrium bond lengths of 19 covalent molecules (22 molecular isomers) from the APW+lo PBE calculations of Tran *et al.* [135], $\Delta l_{\text{MAE}} = 0.009$ ($s = 0.010$, $u_{0.95} = \pm 0.021$) Å and $\delta l_{\text{MAPE}} =$

0.716% ($s = 0.801\%$, $u_{0.95} = \pm 1.661\%$), which are better than but close to the MAE and MAPE values (as well as the corresponding s and $u_{0.95}$ values) for the above 42 bond lengths from our PAW PBE or optB88-vdW calculations.

TABLE III. The MAEs (ΔQ_{MAE}) and MAPEs (δQ_{MAPE}) with standard errors (s) and $u_{0.95}$ values of 42 bond lengths $Q = l$, 15 bond angles $Q = \theta$, 49 formation energies $Q = \Delta H_f$ or ΔH_f^* , and 138 dissociation energies $Q = D$ or D^* from our PAW PBE and optB88-vdW calculations, corresponding to Tables S1, S2, S3, and S4, respectively. For a given quantity Q , the minima (ΔQ_{min} and δQ_{min}) and maxima (ΔQ_{max} and δQ_{max}) of AEs and PEs as well as the minima ($|\Delta Q|_{\text{min}}$ and $|\delta Q|_{\text{min}}$) and maxima ($|\Delta Q|_{\text{max}}$ and $|\delta Q|_{\text{max}}$) of absolute values of AEs and PEs are also listed.

	PBE	optB88	
42 bond lengths	Δl_{MAE}	0.015 Å	0.014 Å
		$s = 0.019$ Å	$s = 0.019$ Å
		$u_{0.95} = \pm 0.038$ Å	$u_{0.95} = \pm 0.037$ Å
	$ \Delta l _{\text{min}}, \Delta l _{\text{max}}$ (Å)	0.005, 0.072	0.000, 0.067
	$\Delta l_{\text{min}}, \Delta l_{\text{max}}$ (Å)	-0.013, 0.072	-0.015, 0.067
	δl_{MAPE}	1.345%	1.228%
		$s = 1.616\%$	$s = 1.542\%$
		$u_{0.95} = \pm 3.262\%$	$u_{0.95} = \pm 3.111\%$
	$ \delta l _{\text{min}}, \delta l _{\text{max}}$ (%)	0.427, 5.768	0.005, 5.374
	$\delta l_{\text{min}}, \delta l_{\text{max}}$ (%)	-1.061, 5.768	-1.339, 5.374
15 bond angles	$\Delta \theta_{\text{MAE}}$	0.446°	0.517°
		$s = 0.601$ °	$s = 0.639$ °
		$u_{0.95} = \pm 1.282$ °	$u_{0.95} = \pm 1.362$ °
	$ \Delta \theta _{\text{min}}, \Delta \theta _{\text{max}}$ (°)	0.004, 1.437	0.002, 1.236
	$\Delta \theta_{\text{min}}, \Delta \theta_{\text{max}}$ (°)	-0.518, 1.437	-0.937, 1.236
	$\delta \theta_{\text{MAPE}}$	0.379%	0.440%
		$s = 0.506\%$	$s = 0.540\%$
		$u_{0.95} = \pm 1.078\%$	$u_{0.95} = \pm 1.151\%$
	$ \delta \theta _{\text{min}}, \delta \theta _{\text{max}}$ (%)	0.003, 1.231	0.001, 1.058
	$\delta \theta_{\text{min}}, \delta \theta_{\text{max}}$ (%)	-0.490, 1.231	-0.906, 1.058
49 formation enthalpies	$\Delta(\Delta H_f)_{\text{MAE}}$	0.325 eV = 31.3 kJ/mol	0.287 eV = 27.7 kJ/mol
		$s = 0.431$ eV = 41.6 kJ/mol	$s = 0.376$ eV = 36.3 kJ/mol
		$u_{0.95} = \pm 0.866$ eV = ± 83.5 kJ/mol	$u_{0.95} = \pm 0.755$ eV = ± 72.9 kJ/mol
	$ \Delta(\Delta H_f) _{\text{min}}, \Delta(\Delta H_f) _{\text{max}}$ (eV)	0.007, 1.075	0.008, 0.959
	$\Delta(\Delta H_f)_{\text{min}}, \Delta(\Delta H_f)_{\text{max}}$ (eV)	-1.075, 0.558	-0.959, 0.489
	$\Delta(\Delta H_f^*)_{\text{MAE}}$	0.109 eV/atom	0.097 eV/atom
		$s = 0.142$ eV/atom	$s = 0.124$ eV/atom
		$u_{0.95} = \pm 0.285$ eV/atom	$u_{0.95} = \pm 0.249$ eV/atom
	$ \Delta(\Delta H_f^*) _{\text{min}}, \Delta(\Delta H_f^*) _{\text{max}}$ (eV/atom)	0.003, 0.358	0.003, 0.297
	$\Delta(\Delta H_f^*)_{\text{min}}, \Delta(\Delta H_f^*)_{\text{max}}$ (eV/atom)	-0.358, 0.279	-0.297, 0.232

	$\delta(\Delta H_f)_{\text{MAPE}}$	19.741%	18.001%
		$s = 37.621\%$	$s = 34.138\%$
		$u_{0.95} = \pm 75.603\%$	$u_{0.95} = \pm 68.604\%$
	$ \delta(\Delta H_f) _{\min}, \delta(\Delta H_f) _{\max} (\%)$	0.252, 150.986	0.387, 128.677
	$\delta(\Delta H_f)_{\min}, \delta(\Delta H_f)_{\max} (\%)$	-150.986, 63.313	-128.677, 57.163
138 dissociation energies	ΔD_{MAE}	0.876 eV = 84.5 kJ/mol	0.860 eV = 83.0 kJ/mol
		$s = 1.017 \text{ eV} = 98.1 \text{ kJ/mol}$	$s = 0.986 \text{ eV} = 95.1 \text{ kJ/mol}$
		$u_{0.95} = \pm 2.010 \text{ eV} = \pm 194.0 \text{ kJ/mol}$	$u_{0.95} = \pm 1.949 \text{ eV} = \pm 188.1 \text{ kJ/mol}$
	$ \Delta D _{\min}, \Delta D _{\max} (\text{eV})$	0.031, 2.752	0.011, 2.680
	$\Delta D_{\min}, \Delta D_{\max} (\text{eV})$	-0.199, 2.752	-0.048, 2.680
	ΔD_{MAE}^*	0.292 eV/atom	0.288 eV/atom
		$s = 0.334 \text{ eV/atom}$	$s = 0.324 \text{ eV/atom}$
		$u_{0.95} = \pm 0.660 \text{ eV/atom}$	$u_{0.95} = \pm 0.641 \text{ eV/atom}$
	$ \Delta D^* _{\min}, \Delta D^* _{\max} (\text{eV/atom})$	0.010, 0.688	0.002, 0.697
	$\Delta D_{\min}^*, \Delta D_{\max}^* (\text{eV/atom})$	-0.066, 0.688	-0.016, 0.697
	δD_{MAPE}	73.674%	52.357%
		$s = 278.412\%$	$s = 141.844\%$
		$u_{0.95} = \pm 550.505\%$	$u_{0.95} = \pm 280.468\%$
$ \delta D _{\min}, \delta D _{\max} (\%)$	1.309, 2730.320	0.247, 830.539	
$\delta D_{\min}, \delta D_{\max} (\%)$	-2730.320, 859.014	-524.383, 830.539	

B. Bond angles

We select 15 bond angles based on the available experimental data in Tables I and II. The AEs ($\Delta\theta$) and PEs ($\delta\theta$) of the corresponding PBE and optB88-vdW values are plotted in Fig. 2. Among these bond angles, the AE or $|\Delta\theta|$ maxima are $\Delta\theta_{\max} = |\Delta\theta|_{\max} = 1.437^\circ$ (PBE) and 1.236° (optB88-vdW) for θ_{000} of triangular OOO or O₃ trimer. The AE minima are $\Delta\theta_{\min} = -0.518^\circ$ (PBE) for θ_{HCO} of triangular HCO and -0.937° (optB88-vdW) for θ_{HNH} of triangular HNH. The $|\Delta\theta|$ minima are $|\Delta\theta|_{\min} = 0.004^\circ$ (PBE) for $\theta_{\text{O}_1\text{NO}_{\text{III}}}$ of planar NO₃ and 0.002° (optB88-vdW) for $\theta_{\text{O}_1\text{NO}_{\text{II}}}$ of planar NO₃.

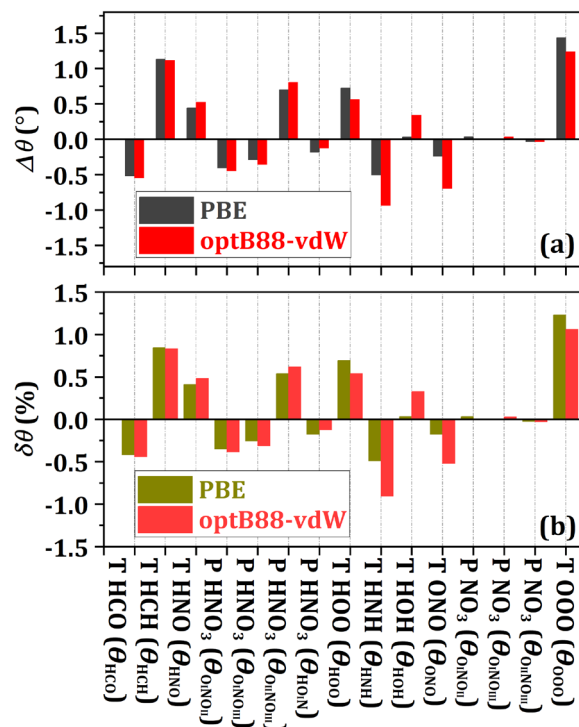


FIG. 2. (a) AEs and (b) PEs of 15 bond angles. On the horizontal axis, “T” denotes “triangular” and “P” denotes “planar”. For original data, see Table S2.

The PE or |PE| maxima are $\delta\theta_{\max} = |\delta\theta|_{\max} = 1.231\%$ (PBE) and 1.058% (optB88-vdW) for θ_{000} of triangular OOO or O₃ trimer. The PE minima are $\delta\theta_{\min} = -0.490\%$ (PBE) and -0.906% (optB88-vdW) for θ_{HNNH} of triangular HNH. The |PE| minima are $|\delta\theta|_{\min} = 0.003\%$ (PBE) for $\theta_{\text{O}_1\text{NO}_{\text{III}}}$ of planar NO₃ and 0.001% (optB88-vdW) for $\theta_{\text{O}_1\text{NO}_{\text{II}}}$ of planar NO₃.

The MAEs (as well as s and $u_{0.95}$ values) of these 15 bond angles are $\Delta\theta_{\text{MAE}} = 0.446^\circ$ ($s = 0.601^\circ$, $u_{0.95} = \pm 1.281^\circ$) (PBE) and 0.517° ($s = 0.639^\circ$, $u_{0.95} = \pm 1.362^\circ$) (optB88-vdW). Correspondingly, the MAPEs (as well as s and $u_{0.95}$ values) are $\delta\theta_{\text{MAPE}} = 0.379\%$ ($s = 0.506\%$, $u_{0.95} = \pm 1.078\%$) (PBE) and 0.440% ($s = 0.540\%$, $u_{0.95} = \pm 1.151\%$) (optB88-vdW). All these errors for bond angles are also listed in Table III.

C. Formation enthalpies and dissociation energies

Based on the available experimental data in Tables I and II, we select 49 formation enthalpies (ΔH_f or ΔH_f^*) and 138 dissociation energies (D or D^*). For definitions of the total formation enthalpy ΔH_f and the per-atom formation enthalpy ΔH_f^* , as well as the total dissociation energy D and the per-atom dissociation energy D^* , see Sec. S1. The AEs [$\Delta(\Delta H_f^*)$ and $\Delta(\Delta H_f)$] and PEs [$\delta(\Delta H_f) = \delta(\Delta H_f^*)$] of the corresponding PBE and optB88-vdW values are plotted in Fig. 3. The AEs (ΔD^* and ΔD) and PEs ($\delta D = \delta D^*$) of the corresponding PBE and optB88-vdW values are plotted in Fig. 4.

For AE or MAE analysis, using ΔH_f^* and D^* is more reasonable than directly using ΔH_f and D because the number of atoms in a molecule can vary (for this work, the number can be 2, 3, 4, or 5), especially for an error comparison between DFT datasets with different samples, e.g., between molecules with varying number of atoms and crystals with different number of atoms in their primitive cells. The per-atom cohesive energies or atomization energies have been widely used for error analysis in the DFT functional tests [16, 127, 129, 130, 132], as analyzed below. Note that the per-atom formation enthalpies are also used in the previous literature, e.g., for comparison between experimental and DFT reaction energies of compounds [136]. Thus, we mainly focus on $\Delta(\Delta H_f^*)$ or ΔD^* [not $\Delta(\Delta H_f)$ or ΔD] for AE or MAE analysis in this work, although all errors are included in Table III. In addition, using ΔH_f^* and ΔH_f or using D^* and D is no distinction for PE or MAPE analysis, according to their definitions in Sec. S1 and Eqs. (1) to (6).

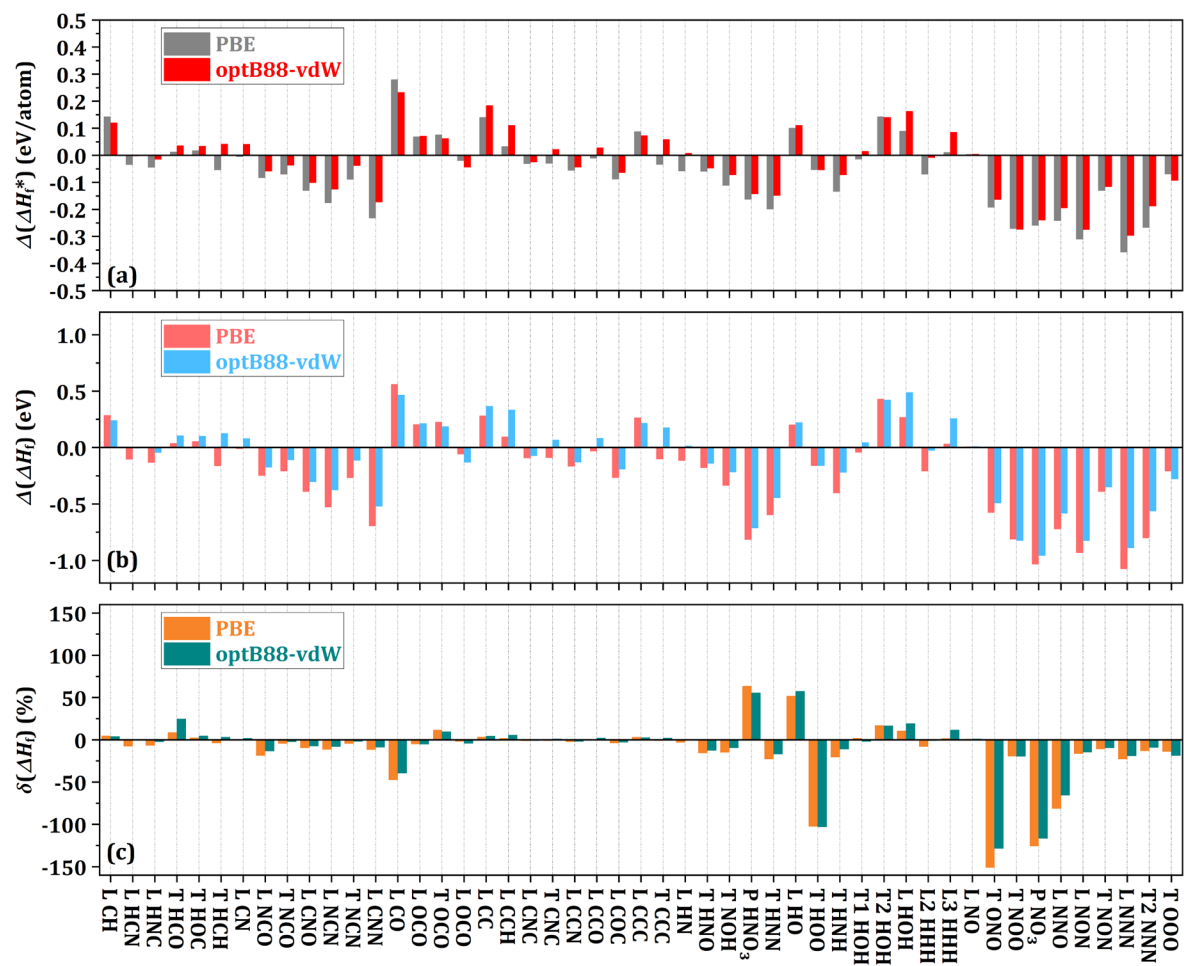


FIG. 3. (a, b) AEs and (c) PEs of 49 formation enthalpies. On the horizontal axis, “L” denotes “linear”, “T” denotes “triangular”, and “P” denotes “planar”. For original data, see Table S3.

Among the 49 formation enthalpies, the AE maxima are $\Delta(\Delta H_f^*)_{\max} = 0.279$ eV/atom (PBE) and 0.232 eV/atom (optB88-vdW) for linear CO. The $|\text{AE}|$ maxima are $|\Delta(\Delta H_f^*)|_{\max} = 0.358$ eV/atom (PBE) and 0.297 eV/atom (optB88-vdW) for linear

NNN. The AE minima are $\Delta(\Delta H_f^*)_{\min} = -0.358$ eV/atom (PBE) and -0.297 eV (optB88-vdW) for linear NNN. The $|AE|$ minima are $|\Delta(\Delta H_f^*)|_{\min} = 0.0034$ eV/atom (PBE) for NO and 0.0027 eV/atom (optB88-vdW) for linear HCN. The MAEs (as well as s and $u_{0.95}$ values) of these 49 formation enthalpies are $\Delta(\Delta H_f^*)_{\text{MAE}} = 0.109$ ($s = 0.142, u_{0.95} = \pm 0.285$) eV/atom (PBE) and 0.097 ($s = 0.124, u_{0.95} = \pm 0.249$) eV/atom (optB88-vdW). The quite small MAE and $u_{0.95}$ values indicate that both PBE and optB88-vdW values for these formation enthalpies are overall satisfactory. In addition, the optB88-vdW result has the smaller MAE and $u_{0.95}$ values than the PBE result and therefore is even better than the PBE result. All above errors are plotted in Fig. 3 and listed in Table III for summary.

As already mentioned above, PE and MAPE can be very sensitive to small AEs when the analyzed data have relatively small magnitudes. For example, the experimental value of ΔH_f^* for triangular HOO is 0.0523 eV/atom and the PAW PBE value is -0.0012 eV/atom. Then, the AE is -0.0535 eV/atom with a quite small magnitude of 0.0535 eV/atom, but the corresponding PE is -102.44% with a huge magnitude $> 100\%$. This implies that PE or MAPE is not very proper for rating the DFT values in the case for which the rated data have relatively small magnitudes and/or the corresponding experimental data perhaps have significant uncertainties, as some of those in the list of the 49 formation enthalpies. Thus, we do not use PE and MAPE to rate our DFT values for formation enthalpies, although we plot them in Fig. 3 and list them in Table III for information only.

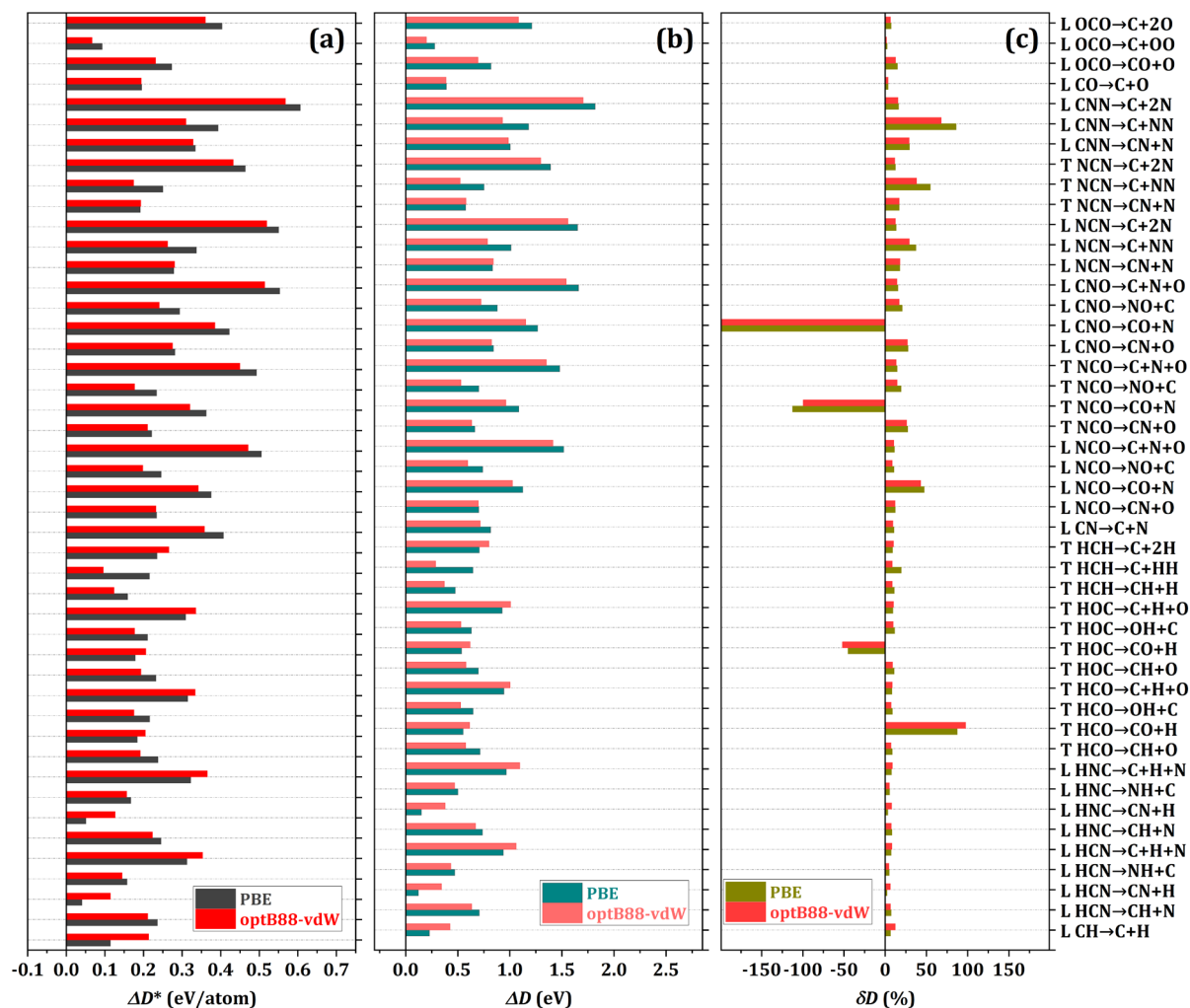


FIG. 4. (a, b) AEs and (c) PEs of 138 dissociation energies (including 51 atomization energies and all bond dissociation energies). On the horizontal axis, “L” denotes “linear”, “T” denotes “triangular”, and “P” denotes “planar”. For original data, see Table S4. Part 1/3

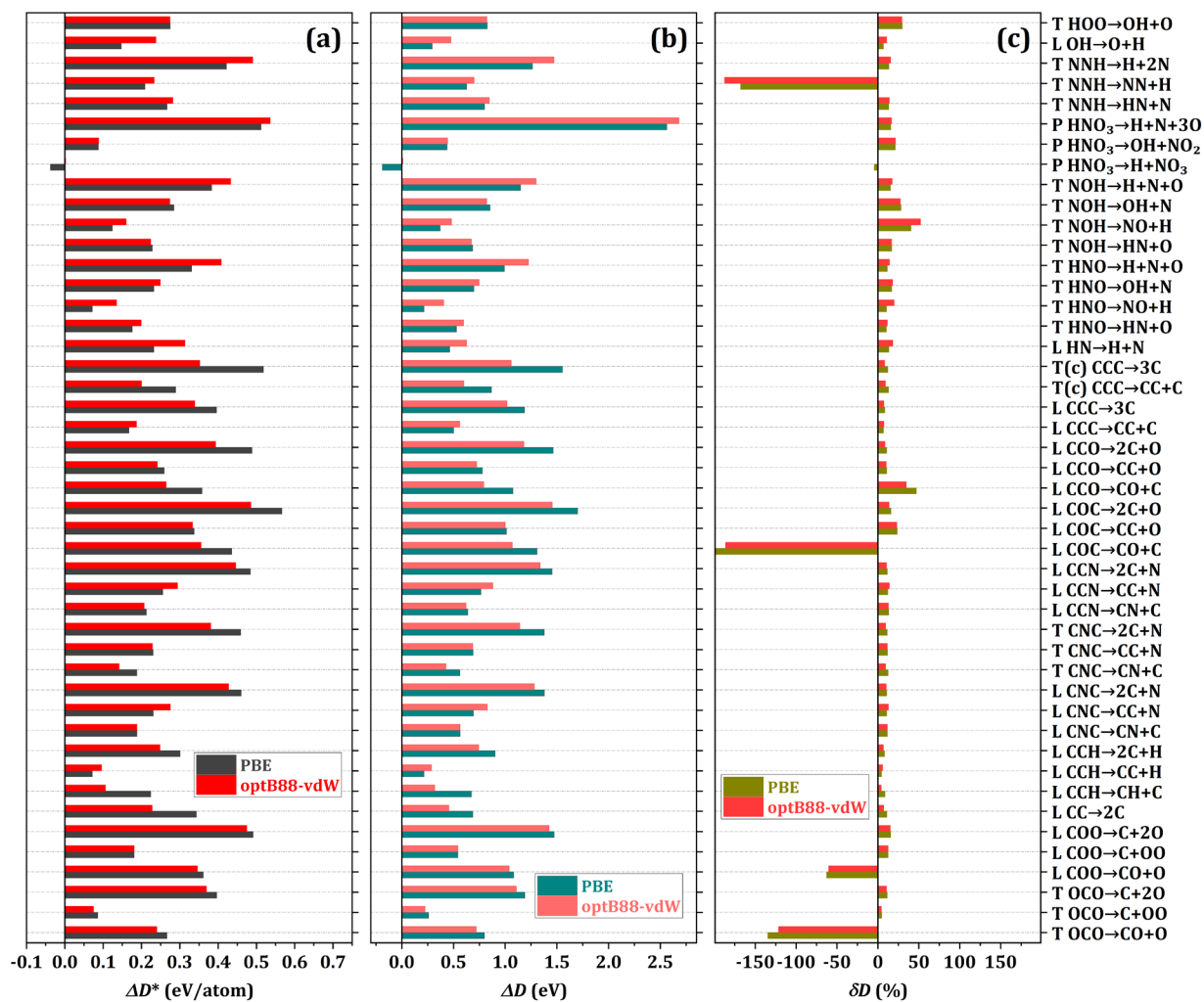


FIG. 4. Continued. Part 2/3.

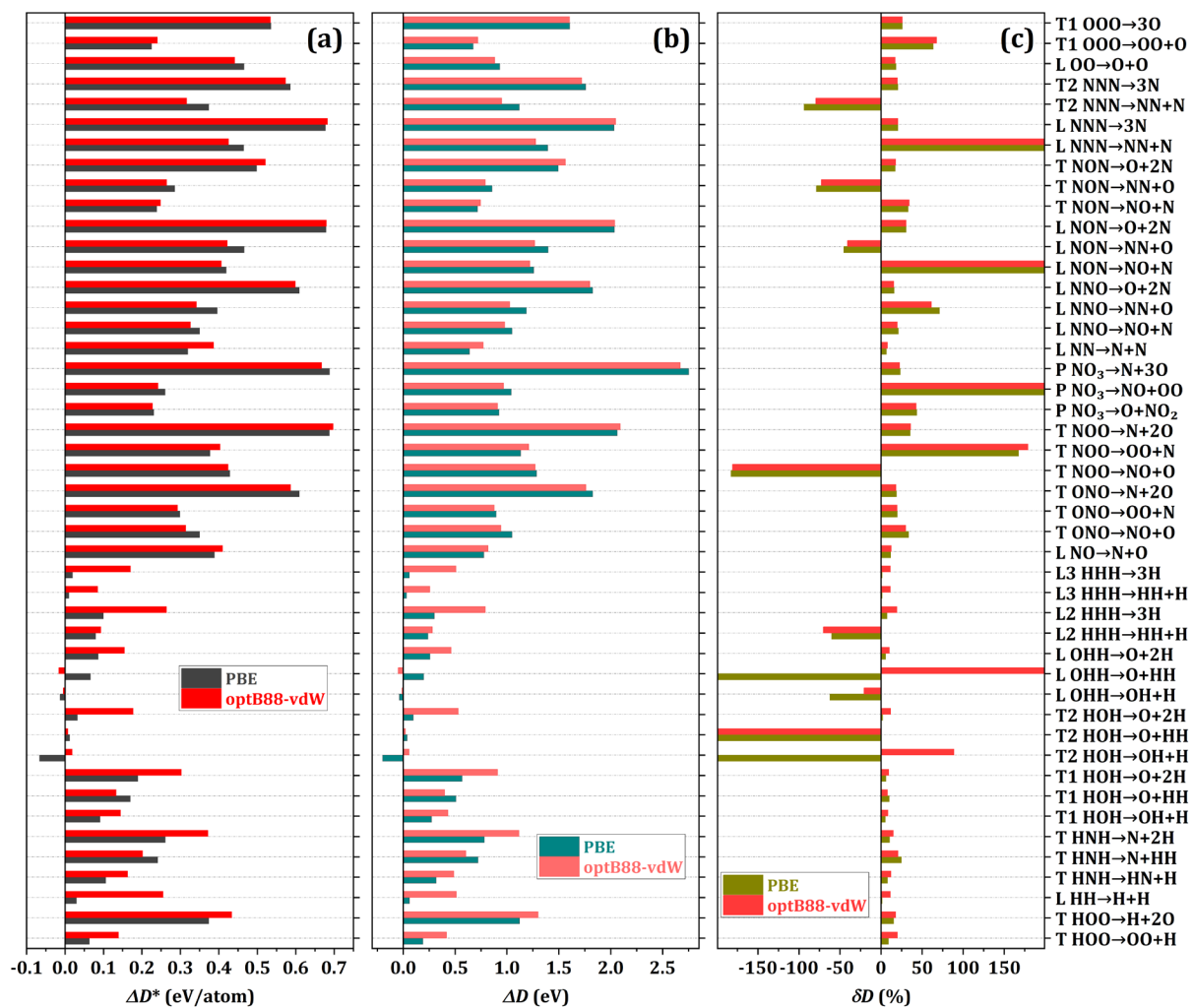


FIG. 4. Continued. Part 3/3

Among the 138 dissociation energies, the AE or |AE| maxima are $\Delta D_{\max}^* = |\Delta D^*|_{\max} = 0.688$ eV/atom (PBE) for the atomization energy of planar NO₃ and 0.697 eV/atom (optB88-vdW) for the atomization energy of triangular NOO. The AE minima are $\Delta D_{\min}^* = -0.066$ eV/atom (PBE) for dissociating O and HH from the triangular vdW complex HOH and -0.016 eV (optB88-vdW) for dissociating O and HH from the linear vdW complex OHH. The |AE| minima are $|\Delta D^*|_{\min} = 0.010$ eV/atom (PBE) for dissociating H and HH from the linear vdW complex HHH and 0.002 eV/atom (optB88-vdW) for dissociating H and NO₃ from the planar HNO₃. The MAEs (as well as s and $u_{0.95}$ values) of these 138 dissociation energies are $\Delta E_{\text{MAE}}^* = 0.292$ ($s = 0.334$, $u_{0.95} = \pm 0.660$) eV/atom (PBE) and 0.288 ($s = 0.324$, $u_{0.95} = \pm 0.641$) eV/atom (optB88-vdW). The quite small MAE and $u_{0.95}$ values indicate that both PBE and optB88-vdW values for these dissociation energies are overall satisfactory. Like the above description for formation enthalpies, some of 138 bond dissociation energies have relatively small magnitudes and/or the corresponding experimental data perhaps have significant uncertainties. Thus, we also do not use PE and MAPE to rate our DFT values for bond dissociation energies, although we list them in Table III for information only. Here, we also note that, among the ΔD^* values for 138 isomers plotted in Fig. 4, there are only 3 and 2 isomers with negative ΔD^* values and these negative ΔD^* values have relatively small $|\Delta D^*|$ values from PBE and optB88-vdW calculations, respectively. This behavior contrasts ΔH_f^* , for which the ratios of numbers with negative and positive values are much lower than those for the ΔD^* values.

In the literature, the error analyses for atomization energies or cohesive energies by testing various types of solids or molecules are available during developing DFT methods. Although these atomization energies or cohesive energies for solids or molecules do not exactly correspond to the formation enthalpies and dissociation energies listed in Table III, making a comparison is still informative. Below, we may as well list the MAEs and MAPEs for atomization energies or cohesive energies of various types of solids or molecules from similar or different PBE or optB88-vdW calculations in the literature. These MAEs (ΔE_{MAE}^* and ΔE_{MAE}) and MAPEs (δE_{MAPE}) with corresponding s and $u_{0.95}$ values are regenerated by using the original data in the literature. Note that all ΔE_{MAE}^* values below always correspond to the atomization or cohesive energies *per atom*. For information, we also list ΔE_{MAE} corresponding to the total atomization energies *per chemical formula or per primitive cell*.

$\Delta E_{\text{MAE}}^* = 0.143$ ($s = 0.198$, $u_{0.95} = \pm 0.396$) eV/atom [$\Delta E_{\text{MAE}} = 0.372$ ($s = 0.478$, $u_{0.95} = \pm 0.957$) eV] and $\delta E_{\text{MAPE}} = 6.569\%$ ($s = 10.327\%$, $u_{0.95} = \pm 20.695\%$) for atomization energies of 55 tested molecules from the PAW PBE calculations of Paier *et al.* [134].

$\Delta E_{\text{MAE}}^* = 0.18$ ($s = 0.25$, $u_{0.95} = \pm 0.53$) eV/atom [$\Delta E_{\text{MAE}} = 0.22$ ($s = 0.29$, $u_{0.95} = \pm 0.60$) eV] and $\delta E_{\text{MAPE}} = 5.09\%$ ($s = 7.20\%$, $u_{0.95} = \pm 15.13\%$) for cohesive energies of 18 tested solids from the PAW PBE calculations of Wu *et al.* [130].

$\Delta E_{\text{MAE}}^* = 0.153$ ($s = 0.203, u_{0.95} = \pm 0.424$) eV/atom [$\Delta E_{\text{MAE}} = 0.351$ ($s = 0.436, u_{0.95} = \pm 0.912$) eV] and $\delta E_{\text{MAPE}} = 7.166\%$ ($s = 11.172\%, u_{0.95} = \pm 23.382\%$) for atomization energies of 19 tested molecules from the APW+lo PBE calculations of Tran *et al.* [135].

$\Delta E_{\text{MAE}}^* = 0.141$ ($s = 0.194, u_{0.95} = \pm 0.389$) eV/atom [$\Delta E_{\text{MAE}} = 0.367$ ($s = 0.469, u_{0.95} = \pm 0.940$) eV] and $\delta E_{\text{MAPE}} = 6.476\%$ ($s = 10.110\%, u_{0.95} = \pm 20.253\%$) for atomization energies of 56 tested molecules from the PAW PBE calculations of Schimka *et al.* [131].

$\Delta E_{\text{MAE}}^* = 0.13$ ($s = 0.17, u_{0.95} = \pm 0.34$) eV/atom [$\Delta E_{\text{MAE}} = 0.18$ ($s = 0.25, u_{0.95} = \pm 0.51$) eV] and $\delta E_{\text{MAPE}} = 4.96\%$ ($s = 6.34\%, u_{0.95} = \pm 13.12\%$) for atomization energies of 23 tested solids from the PAW PBE calculations of Klimeš *et al.* [132].

$\Delta E_{\text{MAE}}^* = 0.07$ ($s = 0.10, u_{0.95} = \pm 0.21$) eV/atom [$\Delta E_{\text{MAE}} = 0.08$ ($s = 0.11, u_{0.95} = \pm 0.22$) eV] and $\delta E_{\text{MAPE}} = 2.91\%$ ($s = 3.89\%, u_{0.95} = \pm 8.04\%$) for atomization energies of 23 tested solids from the PAW optB88-vdW calculations of Klimeš *et al.* [132].

$\Delta E_{\text{MAE}}^* = 0.34$ ($s = 0.41, u_{0.95} = \pm 0.84$) eV/atom [$\Delta E_{\text{MAE}} = 0.34$ ($s = 0.41, u_{0.95} = \pm 0.84$) eV] and $\delta E_{\text{MAPE}} = 8.44\%$ ($s = 11.81\%, u_{0.95} = \pm 24.24\%$) for cohesive energies of 27 transition metals from the PAW PBE calculations of Janthon *et al.* [133].

$\Delta E_{\text{MAE}}^* = 0.19$ ($s = 0.26, u_{0.95} = \pm 0.53$) eV/atom [$\Delta E_{\text{MAE}} = 0.27$ ($s = 0.33, u_{0.95} = \pm 0.67$) eV] and $\delta E_{\text{MAPE}} = 4.99\%$ ($s = 6.35\%, u_{0.95} = \pm 12.80\%$) for cohesive energies of 44 tested solids from the PBE calculations of Tran *et al.* by using the augmented planewave plus local orbitals (APW+lo) method [16].

$\Delta E_{\text{MAE}}^* = 0.13$ ($s = 0.19, u_{0.95} = \pm 0.37$) eV/atom [$\Delta E_{\text{MAE}} = 0.16$ ($s = 0.21, u_{0.95} = \pm 0.42$) eV] and $\delta E_{\text{MAPE}} = 3.82\%$ ($s = 5.31\%, u_{0.95} = \pm 10.71\%$) for cohesive energies of 44 tested solids from the APW+lo optB88-vdW calculations of Tran *et al.* [16].

In contrast to the above list, the results $\Delta(\Delta H_f^*)_{\text{MAE}} = 0.109$ ($s = 0.142, u_{0.95} = \pm 0.285$) eV/atom (PBE) and 0.097 ($s = 0.124, u_{0.95} = \pm 0.249$) eV/atom (optB88-vdW) for 49 formation enthalpies as well as $\Delta D_{\text{MAE}}^* = 0.292$ ($s = 0.334, u_{0.95} = \pm 0.660$) eV/atom (PBE) and 0.288 ($s = 0.324, u_{0.95} = \pm 0.641$) eV/atom (optB88-vdW) for 138 dissociation energies from our PAW DFT calculations are comparably good.

V. SUMMARY

We have performed the PAW DFT calculations for the geometric structures, formation enthalpies, and dissociation energies of 82 molecules or isomers consisting of C, H, N, and/or O. We use PBE and optB88-vdW functionals typically without and with dispersion corrections, respectively. For a convenient comparison and indexing, all results are tabulated (summarized in Tables I and II) together with the corresponding data from previous experiments and AOBM calculations if

available in the literature. Relative to available experimental values, the AEs and PEs of 42 bond lengths, 15 bond angles, 49 formation enthalpies, and 138 dissociation energies from our DFT calculations are illustrated (plotted in Figs. 1, 2, 3, and 4, respectively). The corresponding MAEs and MAPEs for these DFT values are also obtained (summarized in Table III) and compared with the previous error analyses from similar or different planewave DFT methods for various solids and other molecules.

As evaluated in the work, the PAW DFT results for these small molecules is especially informative before calculating various molecular adsorption properties on large-size solid materials often involving the supercells containing hundreds to thousands of atoms, for which using a planewave DFT method is computationally much more efficient than using various existent AOBMs. The data presented in this paper also provide very useful and convenient information for the further development of DFT methods.

SUPPLEMENTARY MATERIAL

See supplementary material for formulation of formation enthalpies and dissociation energies as well as Tables S1, S2, S3, and S4, providing the original data for Figs 1, 2, 3, and 4, respectively.

ACKNOWLEDGEMENTS

The author thanks Prof. James W. Evans and Prof. Theresa L. Windus for their comments and suggestions. The author also thanks Dr. Branko Ruscic for providing the information of ATcT and the uncertainty analysis for DFT datasets. This work was supported by the U. S. Department of Energy (DOE), Office of Science, Basic Energy Sciences, Chemical Sciences, Geosciences, and Biosciences Division. Research was performed at Ames National Laboratory, which is operated by Iowa State University under contract No. DE-AC02-07CH11358. DFT calculations were performed with a grant of computer time at the National Energy Research Scientific Computing Centre (NERSC). NERSC is a DOE Office of Science User Facility supported by the Office of Science of the U. S. DOE under Contract No. DE-AC02-05CH11231. The calculations also partly used the Extreme Science and Engineering Discovery Environment (XSEDE), which is supported by National Science Foundation under Grant No. ACI-1548562.

DATA AVAILABILITY

The data that support the findings of this study are available within the article and its supplementary material and from the corresponding author upon reasonable request.

REFERENCES

- [1] S. Lehtola, *Int. J. Quantum Chem.* **119**, e25968 (2019).
- [2] J. Řezáč, L. Šimová, and P. Hobza, *J. Chem. Theory Comput.* **9**, 364 (2013).
- [3] J. D. Watts and R. J. Bartlett, *Chem. Phys. Lett.* **233**, 81 (1995).
- [4] G. Kresse and J. Furthmüller, *Phys. Rev. B* **54**, 11169 (1996).
- [5] E. J. Bylaska, *Annu. Rep. Comput. Chem.* **13**, 185 (2017).
- [6] P. E. Blöchl, *Phys. Rev. B* **50**, 17953 (1994).
- [7] G. Kresse and D. Joubert, *Phys. Rev. B* **59**, 1758 (1999).
- [8] D. W. Breck, *J. Chem. Educ.* **41**, 678 (1964).
- [9] J. Rouquerol, D. Avnir, C. W. Fairbridge, D. H. Everett, J. H. Haynes, N. Pernicone, J. D. F. Ramsay, K. S. W. Sing, and K. K. Unger, *Pure Appl. Chem.* **66**, 1739 (1994).
- [10] R. Car and M. Parrinello, *Phys. Rev. Lett.* **55**, 2471 (1985).
- [11] J. P. Perdew, K. Burke, and M. Ernzerhof, *Phys. Rev. Lett.* **77**, 3865 (1996).
- [12] Y. Han, K. C. Lai, A. Lii-Rosales, M. C. Tringides, J. W. Evans, and P. A. Thiel, *Surf. Sci.* **685**, 48 (2019).
- [13] V. Baskin, L. Meyer, *Phys. Rev.* **100**, 554 (1955).
- [14] J. Klimeš, D. R. Bowler, and A. Michaelides, *J. Phys. Condens. Matter* **22**, 022201 (2010).
- [15] F. Tran, J. Stelzl, and P. Blaha, *J. Chem. Phys.* **144**, 204120 (2016).
- [16] F. Tran, L. Kalantari, B. Traoré, X. Rocquefelte, and P. Blaha, *Phys. Rev. Mater.* **3**, 063602 (2019).
- [17] J. Klimeš and A. Michaelides, *J. Chem. Phys.* **137**, 120901 (2012).
- [18] S. A. Tolba, K. M. Gameel, B. A. Ali, H. A. Almossalami, and N. K. Allam, "The DFT+U: Approaches, Accuracy, and Applications" In *Density Functional Calculations: Recent Progresses of Theory and Application*, edited by Gang Yang. London: IntechOpen, 2018. DOI: 10.5772/intechopen.72020
- [19] A. Lii-Rosales, Y. Han, J. W. Evans, D. Jing, Y. Zhou, M. C. Tringides, M. Kim, C.-Z. Wang, and P. A. Thiel, *J. Phys. Chem. C* **122**, 4454 (2018).

- [20] A. Lii-Rosales, Y. Han, K. M. Yu, D. Jing, N. Anderson, D. Vaknin, M. C. Tringides, J. W. Evans, M. S. Altman, and P. A. Thiel, *Nanotechnology* **29**, 505601 (2018).
- [21] Y. Han, A. Lii-Rosales, M. C. Tringides, J. W. Evans, and P. A. Thiel, *Phys. Rev. B* **99**, 115415 (2019).
- [22] S. E. Julien, A. Lii-Rosales, K.-T. Wan, Y. Han, M. C. Tringides, J. W. Evans, and P. A. Thiel, *Nanoscale* **11**, 6445 (2019).
- [23] A. Lii-Rosales, Y. Han, K. C. Lai, D. Jing, M. C. Tringides, J. W. Evans, and P. A. Thiel, *J. Vac. Sci. Technol. A* **37**, 061403 (2019).
- [24] A. Lii-Rosales, Y. Han, S. E. Julien, O. Pierre-Louis, D. Jing, K.-T. Wan, M. C. Tringides, J. W. Evans, and P. A. Thiel, *New J. Phys.* **22**, 023016 (2020).
- [25] Y. Han, M. C. Tringides, J. W. Evans, and P. A. Thiel *Phys. Rev. Res.* **2**, 013182 (2020).
- [26] A. Lii-Rosales, Y. Han, D. Jing, M. C. Tringides, and P. A. Thiel, *Phys. Rev. Res.* **2**, 033175 (2020).
- [27] W. Li, L. Huang, M. C. Tringides, J. W. Evans, and Y. Han, *J. Phys. Chem. Lett.* **11**, 9725 (2020).
- [28] Y. Han, J. W. Evans, and M. C. Tringides, *Appl. Phys. Lett.* **119**, 033101 (2021).
- [29] Y. Han, J. W. Evans, and M. C. Tringides, *Phys. Rev. Mater.* **5**, 074004 (2021).
- [30] Y. Han, J. W. Evans, and M. C. Tringides, *J. Vac. Sci. Technol. A* **40**, 012202 (2022).
- [31] Y. Han, P. Chatterjee, S. B. Alam, T. Prozorov, I. I. Slowing, and J. W. Evans, *Phys. Chem. Chem. Phys.* in review (2022).
- [32] M. W. Chase, NIST-JANAF Thermochemical Tables, 4th Edition, *J. Phys. Chem. Ref. Data, Monograph* **9**, 1 (1998).
- [33] B. Ruscic and D. H. Bross, ATcT enthalpies of formation based on version 1.124 of the Thermochemical Network (<https://atct.anl.gov>).
- [34] B. Ruscic, *Int. J. Quantum Chem.* **114**, 1097 (2014).
- [35] B. Ruscic and D. H. Bross, *Aided Chem. Eng.* **45**, 3 (2019).
- [36] A. Kalemios, A. Mavridis, and A. Metropoulos, *J. Chem. Phys.* **111**, 9536 (1999).
- [37] K. P. Huber and G. Herzberg, Constants of Diatomic Molecules, in *Molecular Spectra and Molecular Structure* **4**, Van Nostrand Reinhold Company, New York, 1979.
- [38] M. Zachwieja, *J. Mol. Spectrosc.* **170**, 285 (1995).
- [39] J. M. Bowman, B. Gazdy, J. A. Bentley, T. J. Lee, and C. E. Dateo, *J. Chem. Phys.* **99**, 308 (1993).

- [40] T. van Mourik, G. J. Harris, O. L. Polyansky, J. Tennyson, A. G. Császár, and P. J. Knowles, *J. Chem. Phys.* **115**, 3706 (2001).
- [41] G. Winnewisser, *J. Mol. Spectrosc.* **39**, 149 (1971).
- [42] R. A. Creswell and A. G. Robiette, *Mol. Phys.* **36**, 869 (1978).
- [43] P. S. Peters, D. Duflot, L. Wiesenfeld, and C. Toubin, *J. Chem. Phys.* **139**, 164310 (2013).
- [44] J. A. Austin, D. H. Levy, C. A. Gottlieb, and H. E. Radford, *J. Chem. Phys.* **60**, 207 (1974).
- [45] J. M. Brown and D. A. Ramsay, *Can. J. Phys.* **53**, 2232 (1975).
- [46] J. F. Ogilvie, *J. Mol. Struct.* **31**, 407 (1976).
- [47] E. Hirota, *J. Mol. Struct.* **146**, 237 (1986).
- [48] J. M. Bowman, J. S. Bittman, and L. B. Harding, *J. Chem. Phys.* **85**, 911 (1986).
- [49] W. J. Morgan and R. C. Fortenberry, *Spectrochim Acta A* **135**, 965 (2015)
- [50] P. R. Bunker and P. Jensen, *J. Chem. Phys.* **79**, 1224 (1983).
- [51] P. Jensen and P. R. Bunker, *J. Chem. Phys.* **89**, 1327 (1988).
- [52] H. Yang, T. C. Caves, and J. L. Whitten, *J. Chem. Phys.* **103**, 8756 (1995).
- [53] C. Sun, Y. Liu, B. Xu, Y. Zeng, L. Meng, and S. Zhang, *J. Chem. Phys.* **139**, 154307 (2013).
- [54] S. Andersson, N. Marković and G. Nyman, *Phys. Chem. Chem. Phys.* **2**, 613 (2000).
- [55] D. Koner, R. J. Bemish, and M. Meuwly, *J. Chem. Phys.* **149**, 094305 (2018).
- [56] M. O. Alves, C. E. M. Gonçalves, J. P. Braga, V. C. Mota, A. J. C. Varandas, and B. R. L. Galvão, *J. Chem. Phys.* **154**, 034303 (2021).
- [57] P. Misra, C. W. Mathews, and D. A. Ramsay, *J. Mol. Spectrosc.* **130**, 419 (1988).
- [58] A. Busch, N. González-García, G. Lendvay, and M. Olzmann, *J. Phys. Chem. A* **119**, 7838 (2015).
- [59] N. Faßheber, L. Bornhorst, S. Hesse, Y. Sakai, and G. Friedrichs, *J. Phys. Chem. A* **124**, 4632 (2020).
- [60] J. M. L. Martin, P. R. Taylor, J. P. François, R. Gijbels, *Chem. Phys. Lett.* **226**, 475 (1994).
- [61] L. V. Moskaleva and M. C. Lin, *J. Phys. Chem. A* **105**, 4156 (2001).

- [62] P. I. Nagy, C. W. Ulmer II, and D. A. Smith, *J. Chem. Phys.* **102**, 6812 (1995).
- [63] J. Pacansky, U. Wahlgren, and P. S. Bagus, *J. Chem. Phys.* **62**, 2740 (1975).
- [64] G. Herzberg, *Electronic Spectra and Electronic Structure of Polyatomic Molecules*, in *Molecular Spectra and Molecular Structure 3*, D. Van Nostrand Company, Princeton, New Jersey, 1966.
- [65] C. W. Bauschlicher and S. R. Langhoff, *J. Chem. Phys.* **87**, 2919 (1987).
- [66] M. Hermann and G. Frenking, *Chem. Eur. J.* **22**, 4100 (2016).
- [67] D. Duflot and J-M. Robbe, and J-P. Flament, *J. Chem. Phys.* **100**, 1236 (1994).
- [68] M. Bogey, C. Demuynck, and J. L. Destombes, *Mol. Phys.* **66**, 955 (1989).
- [69] R. Pd. and P. Chandra, *J. Chem. Phys.* **114**, 1589 (2001).
- [70] L. H. Coudert, B. Gans, G. A. Garcia, and J.-C. Loison, *J. Chem. Phys.* **148**, 054302 (2018).
- [71] A. J. Merer and D. N. Travis, *Can. J. Phys.* **43**, 1795 (1965).
- [72] S. T. Brown, Y. Yamaguchi, and H. F. Schaefer III, *J. Phys. Chem. A* **104**, 3603 (2000).
- [73] S. Mishra, W. Domcke, L. V. Poluyanov, *Chem. Phys. Lett.* **446**, 256 (2007).
- [74] V. Zengin, B. J. Persson, K. M. Strong, and R. E. Continetti, *J. Chem. Phys.* **105**, 9740 (1996).
- [75] H. Choi, D. H. Mordaunt, R. T. Bise, T. R. Taylor, and D. M. Neumark, *J. Chem. Phys.* **108**, 4070 (1998).
- [76] M. Mladenović, S. Schmatz, and P. Botschwina, *J. Chem. Phys.* **101**, 891 (1994).
- [77] A. A. Breier, T. Büchling, R. Schnierer, V. Lutter, G. W. Fuchs, K. M. T. Yamada, B. Mookerjee, J. Stutzki, and T. F. Giesen, *J. Chem. Phys.* **145**, 234302 (2016).
- [78] W. P. Kraemer, P. R. Bunker, and M. Yoshimine, *J. Mol. Spectrosc.* **107**, 191 (1984).
- [79] A. M. Mebel, K. Morokuma, and M. C. Lin, *J. Chem. Phys.* **101**, 3916 (1994).
- [80] U. Bozkaya, J. M. Turney, Y. Yamaguchi, and H. F. Schaefer III, *J. Chem. Phys.* **136**, 164303 (2012).
- [81] F. W. Dalby, *Can. J. Phys.* **36**, 1336 (1958).
- [82] L. A. Curtis, D. L. Drapcho, and J. A. Pople, *Chem. Phys. Lett.* **103**, 437 (1984).
- [83] S. F. Selgren, P. W. McLoughlin, and G. I. Gellene, *J. Chem. Phys.* **90**, 1624 (1989).

- [84] S. P. Walch and R. J. Duchovic, *J. Chem. Phys.* **90**, 3230 (1989).
- [85] M. Monge-Palacios, C. Rangel, and J. Espinosa-Garcia, *J. Chem. Phys.* **138**, 084305 (2013).
- [86] Á. Ganyecz, J. Csontos, B. Nagy, and M. Kállay, *J. Phys. Chem. A* **119**, 1164 (2015).
- [87] C. N. R. Rao, G. V. Kulkarni, A. M. Rao, and U. C. Singh, *J. Mol. Struct. Theochem* **108**, 113 (1984).
- [88] C. E. Barnes, J. M. Brown, and H. E. Radford, *J. Mol. Spectrosc.* **84**, 179 (1980).
- [89] K. G. Lubic, T. Amano, H. Uehara, K. Kawaguchi, and E. Hirota, *J. Chem. Phys.* **81**, 4826 (1984).
- [90] F.-M. Tao, *J. Chem. Phys.* **100**, 4947 (1994).
- [91] L. E. Sutton, *Tables of interatomic distances and configuration in molecules and ions, Supplement 1956-1959, Special Publication No. 18* (The Chemical Society, London, 1965).
- [92] R. J. Buenker, M. Peric, S. D. Peyerimhoff, and R. Marian, *Mol. Phys.* **43**, 987 (1981).
- [93] A. R. Hoy and P. R. Bunker, *J. Mol. Spectrosc.* **74**, 1 (1979).
- [94] I. Shavitt, R. M. Stevens, F. L. Minn, and M. Karplus, *J. Chem. Phys.* **48**, 2700 (1968).
- [95] B. Liu, *J. Chem. Phys.* **58**, 1925 (1973).
- [96] W. W. Walters and G. Michalski, *J. Chem. Phys.* **145**, 224311 (2016).
- [97] H. Nakamura and S. Kato, *J. Chem. Phys.* **110**, 9937 (1999).
- [98] J.-L. Teffo and A. Chédin, *J. Mol. Spectrosc.* **135**, 389 (1989).
- [99] R. Tian, J. C. Facelli, and J. Michl, *J. Phys. Chem.* **92**, 4073 (1988).
- [100] A. E. Douglas and W. J. Jones, *Can. J. Phys.* **43**, 2216 (1965).
- [101] C. R. Brazier, P. F. Bernath, J. B. Burkholder, and C. J. Howard, *J. Chem. Phys.* **89**, 1762 (1988).
- [102] L. Jin, X. Yu, J. Pang, S. Zhang, and Y. Ding, *J. Phys. Chem. A* **113**, 8500 (2009).
- [103] Y. Jiang, Y. Shi, X. Xiang, J. Qi, Y. Han, Z. Liao, and T. Lu, *Phys. Rev. Appl.* **11**, 054088 (2019).
- [104] W. J. Orville-Thomas, *J. Mol. Spectrosc.* **3**, 588 (1958).
- [105] P. J. Hay and T. H. Dunning, *J. Chem. Phys.* **67**, 2290 (1977).

- [106] A. Kalemios and A. Mavridis, *J. Chem. Phys.* **129**, 054312 (2008).
- [107] R. Trambarulo, S. N. Ghosh, C. A. Burrus, and W. Gordy, *J. Chem. Phys.* **21**, 851 (1953).
- [108] R. H. Hughes, *J. Chem. Phys.* **24**, 131 (1956).
- [109] T. Tanaka and Y. Morino, *J. Mol. Spectrosc.* **33**, 538 (1970).
- [110] V. G. Tyuterev, S. Tashkun, P. Jensen, A. Barbe, and T. Cours, *J. Mol. Spectrosc.* **198**, 57 (1999).
- [111] A. V. Orden and R. J. Saykally, *Chem. Rev.* **98**, 2313 (1998).
- [112] H. F. King and K. Morokuma, *J. Chem. Phys.* **71**, 3213 (1979).
- [113] G. D. Carney, *J. Chem. Phys.* **72**, 4764 (1980).
- [114] C. Nager and M. Jungen, *Chem. Phys.* **70**, 189 (1982).
- [115] T. Ishiwata, I. Tanaka, K. Kawaguchi, and E. Hirota, *J. Chem. Phys.* **82**, 2196 (1985).
- [116] J. F. Stanton, J. Gauss, and R. J. Bartlett, *J. Chem. Phys.* **94**, 4084 (1991).
- [117] J. F. Stanton, J. Gauss, and R. J. Bartlett, *J. Chem. Phys.* **97**, 5554 (1992).
- [118] J. F. Stanton, *J. Chem. Phys.* **126**, 134309 (2007).
- [119] W. Einfeld and K. Morokuma, *J. Chem. Phys.* **113**, 5587 (2000).
- [120] W. Einfeld, O. Vieuxmaire, and A. Viel, *J. Chem. Phys.* **140**, 224109 (2014).
- [121] A. Lund and K.-Å. Thuomas, *Chem. Phys. Lett.* **44**, 569 (1976).
- [122] U. Kaldor, *Chem. Phys. Lett.* **166**, 599 (1990).
- [123] L. R. Maxwell and V. M. Mosley, *J. Chem. Phys.* **8**, 738 (1940).
- [124] A. P. Cox and J. M. Riveros, *J. Chem. Phys.* **42**, 3106 (1965).
- [125] A. I. Pavlyuchko, S. N. Yurchenko, and J. Tennyson, *J. Chem. Phys.* **142**, 094309 (2015).
- [126] A. V. Terentjev, P. Cortona, L. A. Constantin, J. M. Pitarke, F. D. Sala, and E. Fabiano, *Computation* **6**, 7 (2018).
- [127] D. C. Patton, D. V. Porezag, and M. R. Pederson, *Phys. Rev. B* **55**, 7454 (1997).
- [128] M. Ernzerhof and G. E. Scuseria, *J. Chem. Phys.* **110**, 5029 (1999).

- [129] V. N. Staroverov, G. E. Scuseria, J. Tao, and J. P. Perdew, Phys. Rev. B **69**, 075102 (2004).
- [130] Z. Wu and R. E. Cohen, Phys. Rev. B **73**, 235116 (2006).
- [131] L. Schimka, J. Harl, and Georg Kresse, J. Chem. Phys. **134**, 024116 (2011).
- [132] J. Klimeš, D. R. Bowler, and A. Michaelides, Phys. Rev. B **83**, 195131 (2011).
- [133] P. Janthon, S. Luo, S. M. Kozlov, F. Viñes, J. Limtrakul, D. G. Truhlar, and F. Illas, J. Chem. Theory Comput. **10**, 3832 (2014).
- [134] J. Paier, R. Hirschl, M. Marsman, and G. Kresse, J. Chem. Phys. **122**, 234102 (2005).
- [135] F. Tran, R. Laskowski, P. Blaha, and K. Schwarz, Phys. Rev. B **75**, 115131 (2007).
- [136] G. Hautier, S. P. Ong, A. Jain, C. J. Moore, and G. Ceder, Phys. Rev. B **85**, 155208 (2012).

Supplementary Material

for “An evaluation for geometries, formation enthalpies, and dissociation energies of diatomic and triatomic (C, H, N, O), NO₃, and HNO₃ molecules from the PAW DFT method with PBE and optB88-vdW functionals”

Yong Han

Division of Chemical and Biological Sciences, Ames National Laboratory, Ames, Iowa 50011, USA.

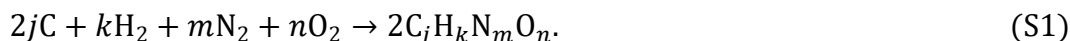
Department of Physics and Astronomy, Iowa State University, Ames, Iowa 50011, USA.

*Email: y27h@ameslab.gov

S1. Formulation of formation enthalpies and dissociation energies

To avoid any confusion, it is necessary to formulate the formation enthalpies and dissociation energies calculated in this work. Experimentally, the standard formation enthalpy of a chemical compound is the change of enthalpy to form the compound from its constituents at the standard states, for which the standard pressure is 100 kPa (101.325 kPa prior to 1982) [32] and the temperature is usually 298.15 K but also 0 K from extrapolation of experimental values at higher temperatures. In the standard DFT calculations, the temperature is always 0 K and the pressure is zero. Under low-pressure condition, the pressure effects can be ignored and thus the formation energies from the DFT calculations [103] can compare with the experimental values of formation enthalpies.

Consider forming a molecule with the chemical formula of C_jH_kN_mO_n containing *j* C atoms, *k* H atoms, *m* N atoms, and *n* O atoms by the reaction



At 0 K, the formation enthalpy ΔH_f is reduced to the formation energy ΔE_f [103] and can be defined as

$$\Delta H_f = \Delta E_f = E_{\text{C}_j\text{H}_k\text{N}_m\text{O}_n} - jE - \frac{k}{2}E_{\text{H}_2} - \frac{m}{2}E_{\text{N}_2} - \frac{n}{2}E_{\text{O}_2}, \quad (\text{S2})$$

where $E_{\text{C}_j\text{H}_k\text{N}_m\text{O}_n}$ is the total energy of the molecule, E is the energy per C atom in bulk graphite, E_{H_2} is the energy of a molecule H₂ in gas phase, E_{N_2} is the energy of a molecule N₂ in gas phase, and E_{O_2} is the energy of a molecule O₂ in gas phase. $\Delta H_f > 0$ indicates that reaction (1) is endothermic (i.e., the product is more unfavorable than the reactants thermodynamically), and $\Delta H_f < 0$ indicates that reaction (1) is exothermic (i.e., the product is more favorable than the reactants thermodynamically). For comparison purposes, the average over all atoms,

$$\Delta H_f^* \equiv \frac{\Delta H_f}{N} = \frac{\Delta H_f}{j + k + m + n}, \quad (\text{S3})$$

is also used in literature [136], where $N = j + k + m + n$ is the total number of atoms in the molecule C_jH_kN_mO_n.

For dissociation of a compound, we can first define a general dissociation energy

$$D_{p_1+p_2+p_3+\dots} = E_{p_1} + E_{p_2} + E_{p_3} + \dots - E_{p_1+p_2+p_3+\dots}, \quad (\text{S4})$$

and the average over all atoms,

$$D_{p_1+p_2+p_3+\dots}^* \equiv \frac{D_{p_1+p_2+p_3+\dots}}{N}, \quad (\text{S5})$$

where p_i labels a product after dissociation, E_{p_i} is the corresponding total energy of the product p_i , and N is the total number of atoms in the molecule before dissociation.

$D_{p_1+p_2+p_3+\dots} > 0$ indicates that the dissociation process is endothermic, and

$D_{p_1+p_2+p_3+\dots} < 0$ indicates that the dissociation process is exothermic. Specifically, if any p_i does not involve any recombination of atoms, i.e., the energy change is only from breaking bonds, then $D_{p_1+p_2+p_3+\dots}$ is called the “bond dissociation energy”. For example, for a most stable H_2O molecule, $D_{\text{H}_2+\text{O}} = E_{\text{H}_2} + E_{\text{O}} - E_{\text{H}_2\text{O}}$ is not the bond dissociation energy because the dissociation reaction $\text{H}_2\text{O} \rightarrow \text{H}_2 + \text{O}$ corresponds to breaking two O-H bonds plus a recombination of two H atoms into H_2 , but $D_{\text{OH}+\text{H}} = E_{\text{OH}} + E_{\text{H}} - E_{\text{H}_2\text{O}}$ is the bond dissociation energy because the dissociation reaction $\text{H}_2\text{O} \rightarrow \text{OH} + \text{H}$ corresponds to only breaking one O-H bond without any recombination of atoms. Also, if all products p_i are isolated single atoms in vacuum, $D_{p_1+p_2+p_3+\dots}$ is called the “atomization energy”, e.g., for the molecule $\text{C}_j\text{H}_k\text{N}_m\text{O}_n$, the atomization energy is

$$D_{j\text{C}+k\text{H}+m\text{N}+n\text{O}} = jE_{\text{C}} + kE_{\text{H}} + mE_{\text{N}} + nE_{\text{O}} - E_{\text{C}_j\text{H}_k\text{N}_m\text{O}_n}, \quad (\text{S6})$$

where $E_{\text{C}_j\text{H}_k\text{N}_m\text{O}_n}$ is the total energy of the molecule before dissociation, E_{C} is the energy of one single C atom in vacuum, E_{H} is the energy of one single H atom in vacuum, E_{N} is the energy of one single N atom in vacuum, and E_{O} is the energy of one single O atom in vacuum. Correspondingly, the average over all atoms

$$D_{j\text{C}+k\text{H}+m\text{N}+n\text{O}}^* \equiv \frac{D_{j\text{C}+k\text{H}+m\text{N}+n\text{O}}}{N} = \frac{D_{j\text{C}+k\text{H}+m\text{N}+n\text{O}}}{j+k+m+n}, \quad (\text{S7})$$

where N is the total number of atoms in the molecule $\text{C}_j\text{H}_k\text{N}_m\text{O}_n$ before dissociation.

Obviously, for a diatomic molecule, the above general dissociation energy, bond dissociation energy, and atomization energy are identical with no distinction.

In the above all equations, the energies $E_{\text{C}_j\text{H}_k\text{N}_m\text{O}_n}$, E , E_{H_2} , E_{N_2} , E_{O_2} , E_{p_i} , E_{C} , E_{H} , E_{N} , and E_{O} can be directly obtained from the DFT calculations, and then the formation enthalpies and dissociation energies can be readily calculated from these equations. For more thermochemical concepts and relevant aspects, the work from Ruscic and Bross [35] is recommended.

S2. DFT and experimental data for Figures

TABLE S1. DFT and experimental data for 42 bond lengths in Fig. 1. “PBE” and “optB88” denote our PAW PBE and optB88-vdW calculations, respectively. “Exp.” denotes the selected values based on available experimental data in Table I. In the first column, “L” denotes “linear”, “T” denotes “triangular”, and “P” denotes “planar”; the bond of two atoms in a molecule is indicated in a parenthesis. l is the bond length, listed in Table I. Δl and δl are the absolute and percentage errors relative to the experimental values by using Eqs. (1) and (4), respectively.

Molecule and bond	PBE l (Å)	optB88 l (Å)	Exp. l (Å)	PBE Δl (Å)	optB88 Δl (Å)	PBE δl (%)	optB88 δl (%)
L CH (C-H)	1.13691448	1.12995479	1.11978600	0.01712848	0.01016879	1.52962056	0.90810098
L HCN (C-H)	1.07490936	1.06992917	1.06549000	0.00941936	0.00443917	0.88404039	0.41663216
L HCN (C-N)	1.16107445	1.15606992	1.15321000	0.00786445	0.00285992	0.68196200	0.24799612
L HNC (N-H)	1.00495238	1.00194864	0.99400000	0.01095238	0.00794864	1.10184869	0.79966167
L HNC (N-C)	1.17739641	1.17279626	1.16890000	0.00849641	0.00389625	0.72687202	0.33332663
T HCO (C-H)	1.13370652	1.12940706	1.11910000	0.01460652	0.01030706	1.30520224	0.92101341
T HCO (C-O)	1.18817237	1.18598664	1.17540000	0.01277237	0.01058664	1.08664069	0.90068393
T HCH (C-H)	1.08485196	1.08164467	1.07530000	0.00955196	0.00634467	0.88830635	0.59003757
L CN (C-N)	1.17680126	1.17326891	1.17180000	0.00500126	0.00146891	0.42680132	0.12535516
L NCO (C-N)	1.23428379	1.22921756	1.20000000	0.03428379	0.02921756	2.85698233	2.43479633
L NCO (C-O)	1.19320045	1.19141508	1.20600000	-0.01279955	-0.01458492	-1.06132297	-1.20936335
L CO (C-O)	1.14310723	1.13932280	1.12832300	0.01478423	0.01099980	1.31028331	0.97488057
L OCO (C-O)	1.17644149	1.17386410	1.16200000	0.01444149	0.01186410	1.24281291	1.02100712
L CC (C-C)	1.31416137	1.30927409	1.24250000	0.07166137	0.06677409	5.76751429	5.37417185
L CCH (C-C)	1.21130840	1.20653041	1.21652000	-0.00521160	-0.00998959	-0.42840222	-0.82116132
L CCH (C-H)	1.07201427	1.06751411	1.04653000	0.02548427	0.02098411	2.43512112	2.00511329
L CNC (N-C)	1.25305366	1.24819807	1.24500000	0.00805366	0.00319807	0.64688042	0.25687307
L CCC (C-C)	1.30183579	1.29477597	1.29471000	0.00712579	0.00006597	0.55037732	0.00509544
L HN (H-N)	1.05062020	1.04854018	1.03620000	0.01442020	0.01234018	1.39164262	1.19090727
T HNO (N-H)	1.07875335	1.07565811	1.09026000	-0.01150665	-0.01460189	-1.05540457	-1.33930357
T HNO (N-O)	1.21681670	1.21710621	1.20900000	0.00781670	0.00810621	0.64654266	0.67048910
P HNOOO (N-O _i)	1.44570519	1.45489016	1.40600000	0.03970519	0.04889016	2.82398222	3.47725156
P HNOOO (N-O _{ii})	1.22309513	1.22328618	1.21100000	0.01209513	0.01228618	0.99877242	1.01454806
P HNOOO (N-O _{iii})	1.20877837	1.20874893	1.19900000	0.00977837	0.00974893	0.81554412	0.81308866
P HNOOO (H-O _i)	0.98328154	0.98258196	0.96400000	0.01928154	0.01858196	2.00015936	1.92758971
L HO (H-O)	0.98683572	0.98623662	0.96966000	0.01717572	0.01657662	1.77131389	1.70952864
T HOO (O-H)	0.99015913	0.98876141	0.97070000	0.01945913	0.01806141	2.00464939	1.86065844
T HOO (O-O)	1.34514436	1.35195563	1.33054000	0.01460436	0.02141563	1.09762644	1.60954418
L HH (H-H)	0.75000311	0.74421851	0.74144000	0.00856311	0.00277851	1.15493014	0.37474462
T HNH (N-H)	1.03475312	1.03738007	1.02400000	0.01075312	0.01338007	1.05010975	1.30664793
T HOH (O-H)	0.97185858	0.97097499	0.95781000	0.01404858	0.01316499	1.46673940	1.37448844
L NO (N-O)	1.16873149	1.16764992	1.15077000	0.01796149	0.01687992	1.56082372	1.46683709
T ONO (N-O)	1.21184450	1.21280586	1.19300000	0.01884450	0.01980586	1.57958948	1.66017291
P NOOO (N-O _i)	1.25076505	1.25227993	1.24000000	0.01076505	0.01227993	0.86814952	0.99031685
P NOOO (N-O _{ii})	1.25095144	1.25236388	1.24000000	0.01095144	0.01236388	0.88318065	0.99708702
P NOOO (N-O _{iii})	1.25088042	1.25240112	1.24000000	0.01088042	0.01240112	0.87745347	1.00009016
L NN (N-N)	1.11294431	1.10870580	1.09768000	0.01526431	0.01102580	1.39059708	1.00446401
L NNO (N-N)	1.14303696	1.13951667	1.12729200	0.01574496	0.01222467	1.39670616	1.08442807
L NNO (N-O)	1.19771079	1.19968798	1.18508900	0.01262179	0.01459898	1.06505032	1.23188887
L NN (N-N)	1.18883831	1.18661634	1.18115000	0.00768831	0.00546634	0.65091690	0.46279795
L OO (O-O)	1.23265402	1.23603023	1.20752000	0.02513402	0.02851023	2.08145786	2.36105677
T OOO (O-O)	1.28437809	1.28938328	1.27276000	0.01161809	0.01662328	0.91282628	1.30608104

TABLE S2. DFT and experimental data for 15 bond angles in Fig. 2. “PBE” and “optB88” denote our PAW PBE and optB88-vdW calculations, respectively. “Exp.” denotes the selected values based on available experimental data in Table I. In the first column, “T” denotes “triangular” and “P” denotes “planar”; the bond angle of three atoms in a molecule is indicated in a parenthesis. $\Delta\theta$ and $\delta\theta$ are the absolute and percentage errors relative to the experimental value of the bond angle θ (listed in Table I) by using Eqs. (1) and (4), respectively.

Molecule and bond angle	PBE θ (°)	optB88 θ (°)	Exp. θ (°)	PBE $\Delta\theta$ (°)	optB88 $\Delta\theta$ (°)	PBE $\delta\theta$ (%)	optB88 $\delta\theta$ (%)
T HCO (H-C-O)	123.91205206	123.88214291	124.43000000	-0.51794794	-0.54785709	-0.41625648	-0.44029341
T HCH (H-C-H)	135.06250720	135.04375287	133.93080000	1.13170720	1.11295287	0.84499398	0.83099098
T HNO (H-N-O)	108.49165754	108.56885822	108.04700000	0.44465754	0.52185822	0.41154085	0.48299187
P HNOOO (O _I -N-O _{II})	115.47244710	115.43281360	115.88000000	-0.40755290	-0.44718640	-0.35170254	-0.38590473
P HNOOO (O _I -N-O _{III})	113.55835260	113.49290460	113.85000000	-0.29164740	-0.35709540	-0.25616812	-0.31365428
P HNOOO (O _{II} -N-O _{III})	130.96920030	131.07428200	130.27000000	0.69920030	0.80428200	0.53673163	0.61739618
P HNOOO (H-O _I -N)	101.96825880	102.02320360	102.15000000	-0.18174120	-0.12679640	-0.17791601	-0.12412766
T HOO (H-O-O)	105.01288446	104.85225819	104.29000000	0.72288446	0.56225819	0.69314839	0.53912953
T HNH (H-N-H)	102.89355581	102.46321828	103.40000000	-0.50644419	-0.93678172	-0.48979129	-0.90597845
T HOH (H-O-H)	104.51116045	104.81690033	104.47760000	0.03356045	0.33930033	0.03212215	0.32475893
T ONO (O-N-O)	133.86015921	133.40281144	134.10000000	-0.23984079	-0.69718856	-0.17885219	-0.51990198
P NOOO (O _I -N-O _{II})	120.03869150	120.00169180	120.00000000	0.03869150	0.00169180	0.03224292	0.00140983
P NOOO (O _I -N-O _{III})	119.99636550	120.03488520	120.00000000	-0.00363450	0.03488520	-0.00302875	0.02907100
P NOOO (O _{II} -N-O _{III})	119.96494300	119.96342290	120.00000000	-0.03505700	-0.03657710	-0.02921417	-0.03048092
T OOO (O-O-O)	118.19115792	117.98988230	116.75420000	1.43695792	1.23568230	1.23075480	1.05836218

TABLE S3. DFT and experimental data for formation enthalpies of 49 isomers in Fig. 3. “PBE” and “optB88” denote our PAW PBE and optB88-vdW calculations, respectively. “Exp.” denotes the selected values based on available experimental data in Table I. In the first column, “L” denotes “linear”, “T” denotes “triangular”, and “P” denotes “planar”. ΔH_f denotes the formation enthalpy for the molecule (or isomer), listed in Table I. $\Delta(\Delta H_f^*)$ [or $\Delta(\Delta H_f)$] and $\delta(\Delta H_f)$ are the absolute and percentage errors relative to the experimental value of the molecule by using Eqs. (1) and (4), respectively.

Molecule	PBE ΔH_f (eV)	optB88 ΔH_f (eV)	Exp. ΔH_f (eV)	PBE $\Delta(\Delta H_f)$ (eV)	optB88 $\Delta(\Delta H_f)$ (eV)	PBE $\Delta(\Delta H_f^*)$ (eV/atom)	optB88 $\Delta(\Delta H_f^*)$ (eV/atom)	PBE $\delta(\Delta H_f)$ (%)	optB88 $\delta(\Delta H_f)$ (%)
L CH	6.42909884	6.38377449	6.14432253	0.28477631	0.23945196	0.14238816	0.11972598	4.63478786	3.89712554
L HCN	1.23957399	1.33594722	1.34401776	-0.10444377	-0.00807055	-0.03481459	-0.00269018	-7.77101118	-6.60047908
L HNC	1.85690199	1.94579985	1.99056163	-0.13365964	-0.04476179	-0.04455321	-0.01492060	-6.71466978	-2.24870130
T HCO	0.46495776	0.53396214	0.42888384	0.03607392	0.10507829	0.01202464	0.03502610	8.41111713	24.50040825
T HOC	2.30362775	2.35198673	2.25163758	0.05199016	0.10034914	0.01733005	0.03344971	2.30899336	4.45671821
T HCH	3.88987897	4.17623322	4.05298911	-0.16311014	0.12324411	-0.05437005	0.04108137	-4.02444053	3.04082026
L CN	4.51499246	4.60640196	4.52638749	-0.01139503	0.08001447	-0.00569752	0.04000724	-0.25174672	1.76773356
L NCO	1.06742555	1.13940081	1.31564039	-0.24821485	-0.17623958	-0.08273828	-0.05874653	-18.86646587	-13.39572587
T NCO	4.45456960	4.55326711	4.66495777	-0.21038818	-0.11169066	-0.07012939	-0.03723022	-4.50996960	-2.39424809
L CNO	3.64502023	3.73136601	4.03481018	-0.38978995	-0.30344417	-0.12992998	-0.10114806	-9.66067634	-7.52065534
L NCN	4.14900736	4.30053794	4.67677304	-0.52776568	-0.37623510	-0.17592189	-0.12541170	-11.28482557	-8.04475857
T NCN	5.73302946	5.88741197	6.00194856	-0.26891910	-0.11453659	-0.08963970	-0.03817886	-4.48052987	-1.90832339
L C NN	5.30762479	5.48384653	6.00402141	-0.69639662	-0.52017488	-0.23213221	-0.17339163	-11.59883641	-8.66377460
L CO	-0.62114207	-0.71507314	-1.17949534	0.55835327	0.46442220	0.27917664	0.23221110	-47.33831946	-39.37465322
L OCO	-3.86994994	-3.86340063	-4.07429804	0.20434810	0.21089741	0.06811603	0.07029914	-5.0155138	-5.17628834
T OCO	2.19754829	2.15756569	1.97232052	0.22522777	0.18524517	0.07507592	0.06174839	11.41943070	9.39224497
L OCO	3.04777224	2.97489724	3.10720804	-0.05943580	-0.13231080	-0.01981193	-0.04103360	-1.91283629	-4.25818938
L CC	8.77985785	8.86477971	8.49875294	0.28110491	0.36602677	0.14055246	0.18301339	3.30760186	4.30682917
L CCH	5.93845302	6.17529586	5.84296066	0.09549236	0.33233519	0.03183079	0.11077840	1.63431468	5.68778763
L CNC	6.87322282	6.89181090	6.96686206	-0.09363924	-0.07505116	-0.03121308	-0.02501705	-1.34406620	-1.07725921
T CNC	7.37512096	7.53087878	7.46538343	-0.09026248	0.06549535	-0.03008749	0.02183178	-1.20908027	0.87732060
L CCN	6.92937168	6.96568999	7.09641543	-0.16704376	-0.13072544	-0.05568125	-0.04357515	-2.35391741	-1.84213347
L CCO	3.87602600	3.99056243	3.90857337	-0.03254737	0.08198906	-0.01084912	0.02732969	-0.83271746	2.09767220
L CCO	6.50136962	6.57493808	6.76786809	-0.26649847	-0.19293001	-0.08883282	-0.06431000	-3.93770183	-2.85067621
L CCC	8.70551620	8.65766895	8.44221585	0.26330035	0.21545310	0.08776678	0.07181770	3.11885358	2.55209184
T CCC	9.21207752	9.49124988	9.31540557	-0.10332805	0.17584431	-0.03444268	0.05861477	-1.10921684	1.88767211
L HN	3.60223384	3.73246261	3.71807810	-0.11584426	0.01438451	-0.05792213	0.00719225	-3.11570262	0.38688021
T HNO	0.96039057	0.99707962	1.13944781	-0.17905724	-0.14236818	-0.05968575	-0.04745606	-15.71438683	-12.49448902
T NOH	1.92155299	2.04135107	2.25795979	-0.33640680	-0.21660872	-0.11213560	-0.07220291	-14.89870631	-9.59311692
P HNO ₃	-2.10680788	-2.00463082	-1.29004064	-0.81676724	-0.71459018	-0.16335345	-0.14291804	63.31329479	55.39284240
T HNN	2.01554166	2.16786137	2.61324695	-0.59770530	-0.44538558	-0.19923510	-0.14846186	-22.87213215	-17.04337877
L HO	0.58643538	0.60729350	0.38641107	0.20002431	0.22088244	0.10001215	0.11044122	51.76464320	57.16255539
T HOO	-0.00374171	-0.00475450	0.15691504	-0.16065676	-0.16166954	-0.05355225	-0.05388985	-102.38454831	-103.02998808
T HNH	1.55454882	1.73946108	1.95801782	-0.40346901	-0.21855674	-0.13448967	-0.07285225	-20.6059263	-11.16214270
T1 HOH	-2.51962122	-2.43275865	-2.47600329	-0.04361793	0.04324464	-0.01453931	0.01441488	1.76162640	-1.74655028
T2 HOH	2.99092661	2.98218990	2.56204746	0.42887915	0.42014244	0.14295972	0.14004748	16.73970361	16.39869861
L HOH	2.83307038	3.05475939	2.56619317	0.26687721	0.48856622	0.08895907	0.16285541	10.39973204	19.03855990
L2 HHH	2.42776063	2.61224404	2.63770663	-0.20994599	-0.02546258	-0.06998200	-0.00848753	-7.95941407	-0.96533035
L3 HHH	2.26871785	2.49365093	2.23764582	0.03107204	0.25600511	0.01035735	0.08533504	1.38860386	11.44082339
L NO	0.94619713	0.94757151	0.93939667	0.00680045	0.00817484	0.00340023	0.00408742	0.72391697	0.87022204
T NO	-0.19487725	-0.10960816	0.38221354	-0.57709079	-0.49182170	-0.19236360	-0.16394057	-150.98648699	-128.67720517
T NOO	3.38878366	3.37830699	4.20167492	-0.81289126	-0.82336793	-0.27096375	-0.27445598	-19.34683857	-19.59618354
P NO ₃	-0.21293888	-0.13645417	0.82292301	-1.03586190	-0.95937718	-0.25896547	-0.23984430	-125.87591819	-116.58164473
L NNO	0.16832708	0.30754591	0.89156557	-0.72323849	-0.58401966	-0.24107950	-0.19467322	-81.12005601	-65.50495883
L NON	4.72217488	4.82848096	5.65370910	-0.93153422	-0.82522814	-0.31051141	-0.27507605	-16.47651482	-14.59622565
T NON	3.25482955	3.29423574	3.64511364	-0.39028409	-0.35087790	-0.13009470	-0.11695930	-10.70704858	-9.62597968
L NNN	3.61229683	3.79732415	4.68713731	-1.07484048	-0.88981316	-0.35828016	-0.29660439	-22.93170465	-18.98414961
T2 NNN	5.27107342	5.50893183	6.07242559	-0.80135218	-0.56349376	-0.26711739	-0.18783125	-13.19657466	-9.27954988
T OOO	1.28733181	1.21761068	1.49666272	-0.20933091	-0.27905204	-0.06977697	-0.09301735	-13.98651217	-18.64495183

